Macromolecules
PERSPECTIVE

Macromolecules **2010**, *43*, 7875–7890 **7875**
DOI: 10.1021/ma101649u

Relaxation Phenomena in Vitrifying Polymers and Molecular Liquids

C. M. Roland

Naval Research Laboratory, Chemistry Division, Code 6120, Washington, D.C. 20375-5342

Received July 22, 2010; Revised Manuscript Received August 31, 2010

ABSTRACT: Recent experimental results on the dynamics of glass-forming materials, particularly polymers, are surveyed. The focus is on aspects of the behavior that are connected to or correlated with structural relaxation. These results include the invariance to thermodynamic conditions (temperature, pressure, volume) of a number of properties—breadth of the relaxation dispersion, number of dynamically correlating molecules, Johari−Goldstein secondary relaxation time, onset of the dynamic crossover, and the product of temperature and specific volume with the latter raised to a material constant—provided the structural relaxation time is maintained constant. Additional salient experimental findings include the correlation of various high-frequency processes, usually measured in the glassy state, with properties of the equilibrium material above T_g. These correlations indicate that the glass transition, although conventionally defined by the relaxation time becoming larger than experimental time scales (> 100 s), has its beginning many orders of magnitude sooner. Also described herein are effects of spatial confinement on the glass transition; these can be dramatic, yet taken *in toto* are rather discombobulating. Such generally observed phenomena must be included in a comprehensive theory or model of the glass transition, since properties intimately connected to structural relaxation cannot be derived separately and be expected to exhibit such correlations by coincidence.

1. Introduction

It has been almost a hundred years since analytical solutions were obtained for Brownian translational diffusion[1] and rotation[2] of liquid molecules whose dynamics are noncooperative. However, when the density becomes sufficiently high that relaxation entails reciprocal motions—neighboring species must make small adjustments in order for a given molecule to move—the dynamics becomes much more complex. Strong intermolecular cooperativity is the hallmark of materials near their glassy state, and unlike the noncooperative dynamics, there is no comprehensive theory of vitrifying liquids. Liquids near T_g are referred to as supercooled, since avoidance of crystallization, often by fast cooling, is necessary for glass formation. For this reason polymers are the prototypical glass-forming material because their crystallization is often slow or, for random copolymers, not possible. One of the oldest terrestrial glasses, dating to 100 million B.C., is amber, a macromolecule formed by polymerization and concomitant vitrification of tree resin.

The importance of the glass transition extends beyond the obvious merit of understanding how chemical structure and the forces between molecules govern their motions. Glassy materials have properties that are path dependent and thus affected by the specific conditions prevailing during their transition through the supercooled regime. The glass transition is also central to performance in certain uses of rubbery polymers. Invariably these are applications for which energy dissipation is a main requirement. The material is designed to undergo its glass transition during service, since this is the viscoelastic regime of maximum energy dissipation. Such applications include the following:

Automotive Tire Treads. When automobile tires roll over wet or rough surfaces, bulk energy dissipation becomes the dominant friction mechanism, and when sliding on low-friction surfaces, deformation of the tread by small (0.01−1 mm^3) asperities governs the skid resistance.[4,5] Optimal wet-skid resistance is achieved by having the viscoelastic response of the tread rubber fall within the glass transition zone in order to maximize conversion of vehicle kinetic energy to heat. The frequency associated with wet skidding is in the range 10^3−10^6 Hz;[6,7] thus, rubbers having high glass transition temperatures (ca. −25 °C) are used to obtain superior wet-skid performance.[8,9]

Armor Coatings. A recent development in military technology is the use of elastomer coatings to enhance the ballistic penetration resistance of armor.[10] A principal mechanism is energy dissipation associated with an impact-induced transition of the coating to the glassy state.[11,12] The strain rate for a bullet striking a surface is on the order of 10^5 s^{-1}, so that a polymer with a sufficiently high, but subambient T_g, attenuates the projectile energy by undergoing the viscoelastic glass transition (Figure 1).

Sonar Attenuation. A similar mechanism is involved when elastomers are used for sound attenuation. For acoustic tiles on submarines used to dampen active sonar, material selection ensures that the polymer has a T_g such that it undergoes its rubber-to-glass transition at the sonar frequency (≥10 kHz) at seawater temperatures.[13] Since mechanical energy absorption (loss modulus and loss tangent) is much larger for shear than bulk strains, the process is enhanced by converting longitudinal sound waves into shear waves.[13]

Arterial Walls. The storage modulus of the protein elastin under physiological conditions is relatively flat up through frequencies around 5 Hz, beyond which there is an upturn due to onset of the glass transition. This rubbery range coincides with the heart rate of mammals, enabling elastin in arteries to elastically restore vessel walls during the relaxation (diastolic) phase of the blood pressure cycle. At higher rates the mechanical loss increases due to the onset of the glass transition. It is believed that the greater damping of elastin in the transition zone serves to attenuate high-frequency perturbations induced by turbulent flow of blood around obstacles such as plaque.[14]

Published on Web 09/10/2010

These examples illustrate the value of studying the glass transition even when there is no interest in glasses *per se*. This article surveys recent experimental results on the glass transition in polymers and molecular liquids, emphasizing general patterns of behavior. Inorganic glasses and colloidal systems are omitted, as this is not intended to serve as a review of the field; these can be found elsewhere.[15−22] Many phenomena, for example polymer blends, are neglected since the purpose is to highlight characteristics that should be addressed by a comprehensive model. To date, the many-body dynamics of vitrifying materials has proven too complicated for a first-principles theory (notwithstanding mode-coupling theory[23−25]). Though even at the model-building stage theories can be useful, there are so many changes associated with vitrification of a liquid that accounting for selected aspects is not overly challenging. The properties described herein should at least provoke further theoretical developments. Since measurements in the vicinity of T_g cannot distinguish between polymers and molecular liquids, the latter are included in the discussion. The glass transition (or α-relaxation) of small molecules comprises orientational and translational degrees of freedom, while the relevant process for polymers is local segmental relaxation, which involves backbone conformational transitions that change the segment orientation by ca. 10°.[26] Displacements over larger length scales are avoided by cooperative rotations of neighboring chain units,[27,28] although the segmental dynamics also underlie global chain motions and thus have a connection to the rheological properties of polymers.

2. Non-Arrhenius Behavior

The most prominent characteristic of the glass transition is the spectacular change in the segmental relaxation time (and related quantities, such as viscosity and diffusion coefficient) that accompanies small variations in temperature. Despite the enormous change in dynamics, the static structure factor remains essentially unchanged (although see ref 29). Figure 2 shows relaxation times and shift factors for atactic polypropylene (*a*-PP) obtained by various experimental methods.[30] A 10% reduction in T near T_g increases τ_α by 10 orders of magnitude; this corresponds to an apparent activation energy comparable to hydrocarbon bond energies. However, the T dependence is non-Arrhenius, so that equations such as the Vogel−Fulcher−Tammann−Hesse (VFTH) equation[31] are used

$$\tau_\alpha = \tau_0 \exp\left(\frac{B}{T - T_V}\right) \quad (1)$$

where τ_0 and B are material constants. Equation 1 predicts a divergence at T_V, which is sometimes identified with an "ideal" glass transition,[32,33] although its existence is questionable[34−39] and alternative equations have been proposed that avoid it.[40−42] As discussed in section 3.2, the applicability of the VFTH equation above T_g is limited to temperatures up to a characteristic T_B, above which different values of τ_0 and B are required to fit $\tau_\alpha(T)$. Eventually at higher temperatures the behavior becomes Arrhenius. Because of the non-Arrhenius nature in the supercooled regime, "fragility" (proportional to the activation energy at T_g expressed in units of RT[43]) is commonly used to quantify the effect of temperature.

Over the initial several decades change of τ_α, the effect of temperature on segmental relaxation is much stronger than its effect on the global dynamics; only at higher temperatures do the T dependences become equivalent. This difference in the temperature dependence of segmental and chain relaxation times, which causes a breakdown of time−temperature superpositioning in the transition zone,[44−47] is neglected in most theories of polymer rheology. The usual assumption is that a single monomeric friction factor governs both the local and global dynamics.[48−50] Interestingly, it was recently discovered[51] that when plotted logarithmically versus T_g/T (the fragility format appropriate for segmental relaxation[43]), *global* relaxation times for certain polymers, notably polystyrene (PS), collapse to yield an almost universal curve for different molecular weights, notwithstanding the nonlinear dependence of these relaxation times on chain length. The effect is unexplained and absent entirely in most polymes.[52]

The slowing of the dynamics on approach to T_g has been known for many decades, and substantial experimental efforts have been devoted recently to determining the cause or at least the control parameters. There are two direct effects of reducing temperature: the available energy decreases, making it more difficult for segments to surmount minima in the potential energy surface; this trapping of configurations slows the dynamics. Simultaneously, there is a volume decrease, which causes steric constraints (jamming) of the motions. The latter mechanism is the basis for free volume models, which have a long history in the polymer community.[48,53,54] To quantify the respective contributions of thermal energy and density, measurements are carried out as a function of pressure, as well as temperature, with the equation of state for the material used to compute the apparent activation energy at constant volume

$$E_V(T,V) = R\left.\frac{\partial \ln \tau_\alpha}{\partial T^{-1}}\right|_V$$

as well as the usual constant pressure activation enthalpy

$$E_P(T,P) = R\left.\frac{\partial \ln \tau_\alpha}{\partial T^{-1}}\right|_P$$

Mike Roland was born in Trenton, NJ, and received his PhD in chemistry from the Pennsylvania State University in 1980 under the direction of W. A. Steele. He worked at the Firestone Central Research Laboratories in Akron, OH, until 1986, when he joined the Naval Research Laboratory, where he is head of the Polymer Physics Section. From 1991 to 1999 he edited *Rubber Chemistry & Technology*. He was the recipient of the Sparks−Thomas (1991) and Melvin Mooney (2002) awards from the ACS Rubber Division and is a Fellow of the Institute of Materials, Minerals, and Mining (UK). His research interests include the mechanical and viscoelastic properties of materials. He is the author of *Viscoelastic Behavior of Rubbery Materials*, to be published by Oxford University Press in the spring of 2011.

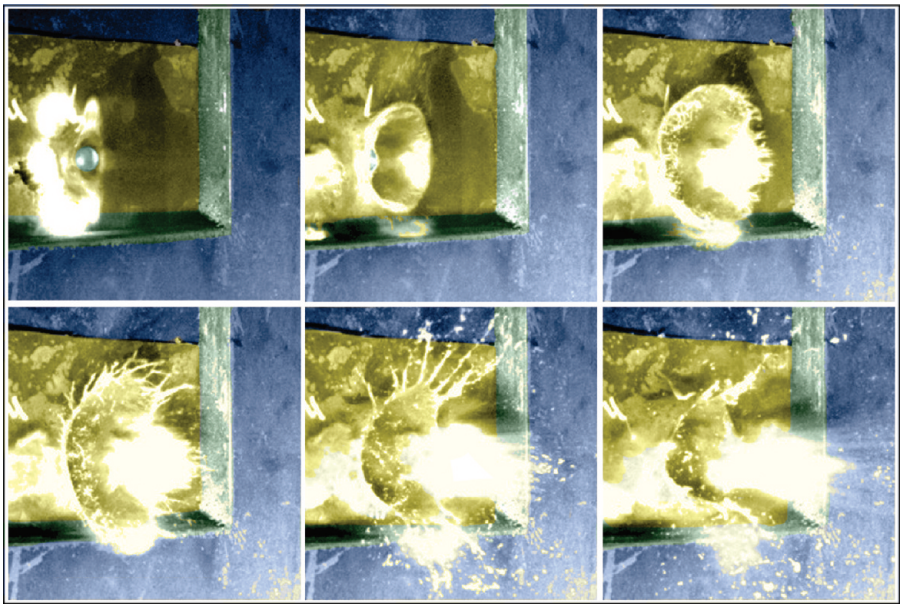

Figure 1. Viscoelastic phase transition induced in an elastomeric polyurea by impact of a 0.50 caliber bullet (seen entering the target in the upper left panel). The material has a calorimetric $T_g = -60$ °C; however, the transition occurs at room temperature due to the high strain rate, $\sim 10^5$ s^{-1} (estimated as the ratio of the projectile velocity to the elastomer thickness). Before and after the impact, the polyurea is a cross-linked, rubbery solid.

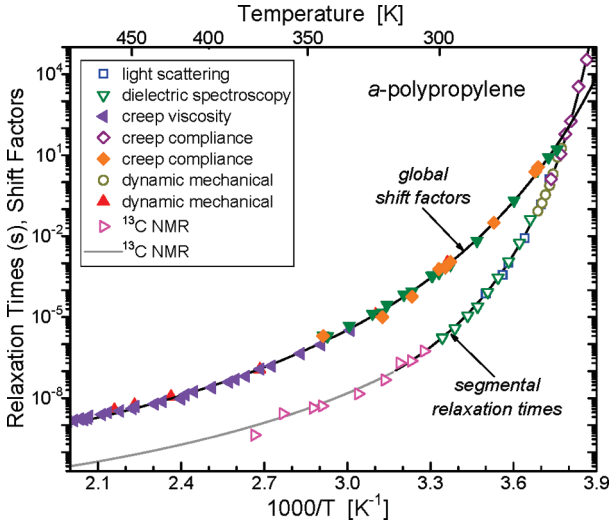

Figure 2. Atactic polypropylene local segmental relaxation times (hollow symbols) and terminal time−temperature shift factors (filled symbols) determined by the indicated experimental methods. Vertical shifting was applied to bring the data into coincidence, whereby the crossing of the curves at low temperature has no meaning (chain relaxation times are always longer than τ_α). From ref 30 and references therein.

Their ratio, E_V/E_P, which varies between zero (density-driven dynamics) and unity (thermally activated dynamics), provides a measure of the relative contribution of temperature and volume to the non-Arrhenius behavior of τ_α.[19,55,56]

In Table 1 this ratio at T_g and $P = 0.1$ MPa is listed for 19 polymers.[19] With one exception (poly(phenylene oxide), which has an unusually high $T_g = 189$ °C for a flexible chain polymer), $E_V/E_a > 0.5$. This means that temperature more strongly influences the segmental dynamics than density, which argues against a free volume interpretation of polymer dynamics. For van der Waals molecular liquids E_V/E_P ratios tend to be smaller, indicative of a stronger effect of density on $\tau_\alpha(T)$.[19] The reason for the different behavior of simple liquids and polymers is that pressure has a negligible effect on the dimensions of a chain molecule (instead, it increases chain interpenetration); thus, interactions among directly bonded segments, which of course are more profuse in polymers than small molecules, remain largely unaffected by changes in volume. In molecular liquids, on the other hand, most near-neighbor interactions are intermolecular, and these are sensitive to density. This influence of intramolecular bonds is apparent in the increase in E_V/E_a with degree of polymerization (Table 2).[57−59]

Table 1. Activation Energy Ratio and Scaling Exponent for Various Polymers at T_g

polymer	T_g	E_V/E_P	γ
poly(phenylene oxide)	189	0.25	
poly(methylphenylsiloxane)	248	0.52	5.6
poly(methyltolylsiloxane)	261	0.55	5.0
poly(vinyl acetate)	302	0.6	2.6
diglycidyl ether of bisphenol A	413	0.6	2.8
poly(phenol glycidyl ether)-*co*-formaldehyde	258	0.63	3.5
polystyrene	373	0.64	2.5
poly[(*o*-cresyl glycidyl ether)-*co*-formaldehyde]	285	0.65	3.3
poly(propylene glycol)	210	0.67	2.5
poly(vinyl methyl ether)	250	0.69	2.9
polyvinylethylene	253	0.70	1.9
poly(cyclohexyl methacrylate)	349	0.72	2.5
poly(α-methylstyrene)	341	0.56	2.7
poly(2-vinylpyridine)	337	0.72	
poly(methyl methacrylate)	380	0.74	1.8
polyoxybutylene	199	0.75	2.7
1,4-polyisoprene	201	0.76	3.0
poly(2-chlorostyrene)	399	0.61	2.6
poly(vinylphenol)	473	0.77	
poly(4-vinylpyridine)	399	0.77	
poly(vinyl ethyl ether)	241	0.81	

3. Properties Invariant to Thermodynamic Conditions

A focus of theoretical efforts is to obtain an expression for τ_α in terms of entropy, free volume, dynamic heterogeneity, or other quantity that might govern the dynamics. Other relaxation properties respond to changes in thermodynamic conditions, and of course these also have to be addressed by theory. Since different combinations of temperature and pressure can yield the same τ_α, due to their compensating effects on molecular mobility,

if there are other properties remaining constant when T and P are changed at fixed τ_α, these properties must have the same control parameter as τ_α. Thus, relations for τ_α and such properties cannot be derived independently; a satisfactory theory must account for their interdependence. Properties remaining constant when τ_α is constant include the following:

3.1. Relaxation Dispersion. The local segmental relaxation peak, or α-dispersion, usually broadens as temperature is lowered toward T_g.[60−64] (In a few materials the peak breadth is invariant to T,[65−67] while in 1,4-polybutadiene (PB) it narrows on approach to T_g, an artifact of an increasing encroachment of an intense secondary relaxation.[68]) A metric of the nonexponentiality ("stretching") of the relaxation is the exponent, β_K, of the Kohlrausch−William−Watts function[69]

$$\Phi(t) = \exp[-(t/\tau_K)^{\beta_K}] \quad (2)$$

where $\Phi(t)$ is a linear susceptibility and the KWW time constant $\tau_K \leq \tau_\alpha$, when the latter is defined as the inverse of the frequency of the peak maximum. As an example, reducing the temperature of poly(cyclohexyl methacrylate) (M_w = 3.4 kg/mol) from 436 to 350 K, which increases τ_α from 3 μs to about 6 min, broadens the α-peak in the dielectric loss from less than 2.2 to 2.8 decades (full width at half-maximum).[70] This corresponds to a decrease in β_K from 0.51 to 0.39, smaller β_K denoting a broader peak.[71] For exponential (Debye) relaxation $\beta_K = 1$, and the peak breadth is 1.14 decades.

Table 2. Effect of Degree of Polymerization on E_V/E_P

liquid	N	E_V/E_P
poly(methyl methacrylate)	3	0.63
	4	0.63
	10	0.63
	1500	0.74
polystyrene	132	0.52
	231	0.54
	332	0.64
	865	0.66
poly(2-vinylpyridine)	48	0.61
	124	0.61
	329	0.64
	857	0.66
poly(4-vinylpyridine)	19	0.62
	152	0.77

If a temperature change is accompanied by a change in pressure, so that τ_α remains constant, the shape of the segmental relaxation peak is also constant.[72,73] This is illustrated in Figure 3 for PCHMA and three other polymers. For various combinations of T and P, the peak breadth is determined only by the frequency of the peak maximum. This temperature−pressure superpositioning of the α-dispersion at fixed τ_α is general, having been found not only for polymers but also molecular liquids, encompassing materials with different physical and chemical structures and different sensitivities to temperature and density. This interdependence of $\tau_\alpha(T,P)$ and $\beta_K(T,P)$ is an outstanding challenge to understanding the glass transition.[73,74]

3.2. Dynamic Crossover. As the relaxation time becomes longer with cooling or densification, certain changes in behavior arise at a characteristic temperature, T_B, which is 10−50% higher than T_g. The cause of this "dynamic crossover" is not entirely clear. It is loosely ascribed to the onset of intermolecular cooperativity; however, above T_B the relaxation dispersion and $\tau_\alpha(T)$ remain nonexponential and non-Arrhenius, respectively. Changes associated with the dynamic crossover include the following: (i) The structural relaxation peak, which is exponential only at very high temperatures, begins to broaden more rapidly as temperature is lowered below T_B, indicative of growing intermolecular cooperativity.[60,75] (ii) The non-Arrhenius behavior changes from a temperature dependence of τ_α described by one set of values of τ_0 and B (eq 1) to a second.[76] (iii) Extrapolation of the relaxation times for the Johari−Goldstein secondary process (see section 5.1), τ_{JG}, intersects the slower α-relaxation times at T_B.[77,78] This extrapolation is questionable because the

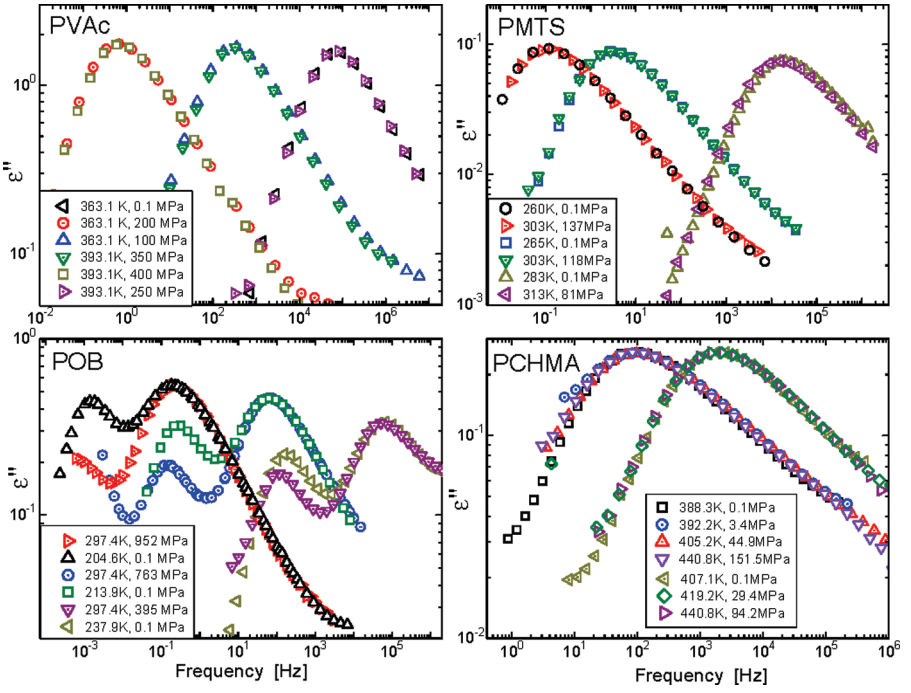

Figure 3. Dielectric α-loss peaks at the indicated state points, showing the superposition of the normalized α-dispersion for constant τ_α: (upper left) poly(vinyl acetate); (lower left) polyoxybutylene; (upper right) polymethyltolylsiloxane; (lower right) poly(cyclohexyl methacrylate). The ordinate values at higher P are normalized to the maximum of the corresponding loss peak at ambient pressure. Data from refs 70 and 73.

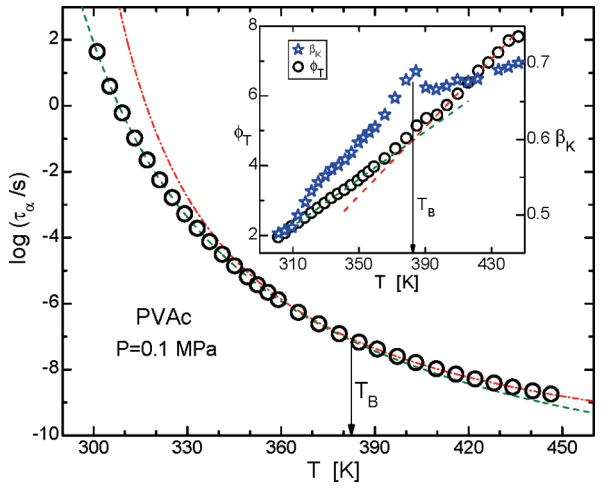

Figure 4. Local segmental relaxation times for poly(vinyl acetate), along with the fit of eq 1 at lower T (log τ_0 (s) = −13.25; B = 1955 K; T_V = 244.0 K) and higher temperatures (log τ_0 (s) = −11.59; B = 1124 K; T_V = 274.7 K). The inset shows the derivative plot used to determine the dynamic crossover at T_B = 383 K (circles), along with the nonexponentiality parameter (stars). From ref 62.

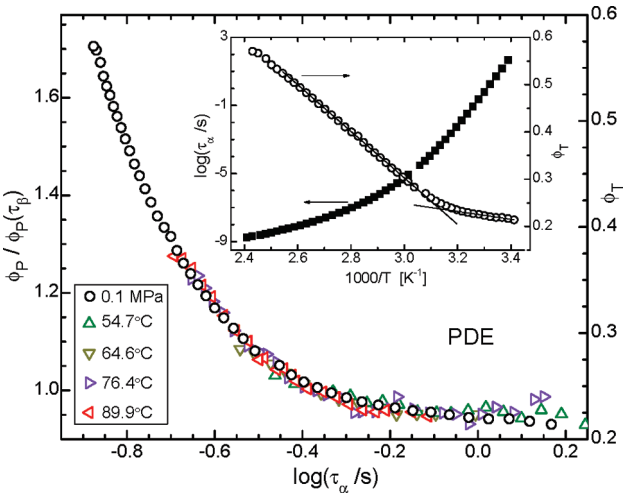

Figure 5. Pressure derivative function (eq 4) normalized by its value at $T_B(P)$, along with ϕ_T for ambient pressure, as a function of log τ_α. The collapse of the curves results from the invariance to pressure of the relaxation time at the dynamic crossover. The inset shows as a function of inverse T the relaxation times at P = 0.1 MPa, along with the corresponding ϕ_T, linear fits of which intersect at $\tau_\alpha(T_B) = 5 \times 10^{-4}$ s. Ambient pressure data from ref 61 and high pressure data from ref 91.

Arrehenius behavior of $\tau_{JG}(T)$ changes near T_g;[79−82] nevertheless, the putative merging of the two relaxations would occur in the vicinity of T_B. (iv) Deviations from the Stokes−Einstein relation, predicting inverse proportionality between viscosity and translational diffusion[83,84] and the Maxwell relation between the viscosity and relaxation times,[85,86] become apparent at T_B. These effects are only observed for small molecules, since the viscosity of polymers is dominated by the chain dynamics. For polymers departures from the Debye−Stokes−Einstein equation,[61] relating rotational and translational motions, are observed in comparisons of $\tau_\alpha(T)$ to the conductivity of free ions[87,88] and the translational and rotational dynamics of probes dissolved in polymers.[89,90]

The dynamic crossover is illustrated for poly(vinyl acetate) in Figure 4,[62] showing segmental relaxation times and their Stickel derivative function[61,76]

$$\phi_T \equiv \left[\frac{-\partial \ln \tau_\alpha}{\partial T}\right]^{-1/2} = \frac{T - T_V}{\sqrt{B}} \qquad (3)$$

The function linearizes τ_α data to bring out the change in dynamics at T_B, equal to 383 K for PVAc in Figure 4. There are similar changes at T_B in β_K (Figure 4) and the dielectric strength.[62]

The data for PVAc in Figure 4 are at ambient pressure (0.1 MPa). Because the relaxation time at the dynamic crossover is usually short ($\tau_\alpha(T_B) \sim 80$ ns in Figure 4), there have been relatively few determinations of the dynamic crossover at elevated pressure, since dielectric measurements at high P become problematic for frequencies beyond about 10^6 Hz due to cable resistance and inductance. Nevertheless, the dynamic crossover can be effected by isothermal variation of pressure, with the pressure counterpart of eq 3

$$\phi_P \equiv \left[\frac{-\partial \ln \tau_\alpha}{\partial P}\right]^{-1/2} \qquad (4)$$

Direct measurements are available for only the few materials having rather long $\tau_\alpha(T_B)$[91] or from viscosity measurements,[92,93] the latter limited to molecular liquids. Results are shown in Figure 5 for phenolphthalein−dimethyl ether (PDE).[91] Varying either pressure at fixed T or temperature at fixed P, the value of T_B changes; however, the relaxation time at $T_B(P)$ is constant.

By exploiting the scaling property of τ_α (section 4), it can be shown that[94]

$$T_B(P) = -(\alpha_\tau \gamma)^{-1} \qquad (5)$$

in which α_τ is the thermal expansion coefficient at constant τ_α evaluated in eq 5 at T_B and γ is the scaling exponent (eq 13), a material constant. Using this relation, T_B for PVAc at ambient pressure is calculated to be 381 K, consistent with the experimental value. Using the same scaling relation, τ_α can be calculated for any $T_B(P)$, and its value, 8×10^{-8} s, is found to be independent of pressure. This invariance of $\tau_\alpha(T_B)$ has been shown for a variety of liquids and polymers.[95] Although the value is a material constant, $\tau_\alpha(T_B)$ is not universal, varying by several orders of magnitude among different materials.[78,95,96]

3.3. Dynamic Heterogeneity. The many-body dynamics of structural relaxation, involving more than one molecule or chain segment, is necessarily intermolecularly correlated. Regions of fast-moving molecules coexist with slow-moving regions, and these spatial variations in mobility persist for times commensurate with τ_α. The heterogeneous dynamics defines a length scale, ξ, within which molecular rearrangements (rotations or translations) occur coordinately with other molecules within their local environment. As temperature is reduced or the density increases, ξ becomes larger, leading ultimately to vitrification as the number of molecules that must be accommodated to permit motion becomes overly large. Classical theories of the glass transition such as the Adam−Gibbs entropy model[97] and free volume approaches,[53] as well as other treatments,[20,98−105] invoke the growth of a dynamic correlation size as the cause of the slowed dynamics near T_g. Since increased heterogeneity implies more dispersive dynamics and hence a broader relaxation peak, it follows from the $T-P$ superpositioning of the peak at fixed τ_α (section 3.1) that ξ or the number dynamically correlated molecules, N_c, should also be constant at fixed τ_α.

Experimentally quantifying the size of the dynamic heterogeneities is difficult because both spatial and temporal

correlations are involved.[106] Information is required about the density simultaneously at two positions and two times, whereas conventional relaxation experiments measuring a linear susceptibility provide only a two-point time correlation function. The spatial extent of the fluctuations over a time span t can be characterized using a four-point susceptibility defined as[104,107]

$$\chi_4(t) = \int \langle \rho(r_1,0)\rho(r_1+r_2,0)\rho(r_1,t)\rho(r_1+r_2,t)\rangle_{r_1} \, dr_2 \tag{6}$$

This quantity describes the probability that if correlation between particles is lost over a time t at position r_1, the same decorrelation transpires within this time interval at r_2. As molecules escape over time from cages formed from the local liquid structure, strong dynamic correlations develop and $\chi_4(t)$ grows. At $t \sim \tau_\alpha$, $\chi_4(t)$ exhibits a maximum, χ_4^{max}, that is proportional to the number of molecules or polymer repeat units dynamically correlated over this time span. Commonly it is assumed that $\xi \sim N_c^{1/3}$, although the dynamic correlation volume has a complex shape that cannot be adequately described by a single length scale.[108] $\chi_4(t)$ can by computed from molecular dynamics (MD) simulations,[109−112] for example as the variance of the self-intermediate scattering function $F_s(\tilde{k},t)$

$$F_s(\tilde{k},t) = N^{-1}\langle \rho_{\tilde{k}}(t)\rho_{-\tilde{k}}(0)\rangle \tag{7}$$

and

$$\chi_4(t) \sim [\langle f_s^2(\tilde{k},t)\rangle - F_s^2(\tilde{k},t)] \tag{8}$$

where $\tilde{k}$ is the wave vector and $f_s(\tilde{k},t)$ represents the instantaneous value, $F_s(\tilde{k},t) = \langle f_s(\tilde{k},t)\rangle$.

The expected connection between the magnitude of the dynamic heterogeneities and the dispersity of the relaxation means that the correlation volume should be invariant for state points for which τ_α is constant, since the normalized relaxation peaks superpose for fixed τ_α (Figure 3). MD simulations in which T and ρ are varied to give state points of constant τ_α bear this out: N_c ($\propto \chi_4^{max}$) is a single function of τ_α (Figure 6[112]). Actually not only χ_4^{max} but also the full time dependence of $\chi_4(t)$ superposes for fixed τ_α, independent of temperature and density.

Experimental determinations of ξ for real materials are limited. Four-dimensional solid-state NMR experiments combine determinations of orientational relaxation times of segments with spin-diffusion measurements to obtain a dynamic correlation length.[113,114] Donth[115] analyzed dynamic heterogeneity by interpreting the magnitude of fluctuations in temperature in terms of the size of the region of correlated motions.[115,116] Kremer et al.[117] characterized ξ by measuring structural relaxation of samples contained in pores of various size, with a change in temperature dependence of τ_α observed for pores having a size commensurate with ξ. Since inhomogeneities in the liquid are frozen below the glass transition, Hong et al.[118] have suggested that the structural heterogeneities intrinsic to the glassy state of amorphous solids can be identified with the dynamic heterogeneity above T_g, providing a means to characterize ξ from properties of the Boson peak.

An appealing method to quantify dynamic correlation was proposed by Berthier et al.,[108,119] who derived an approximation for $\chi_4(t)$ in terms of the temperature derivative of the experimentally accessible, two-point dynamic

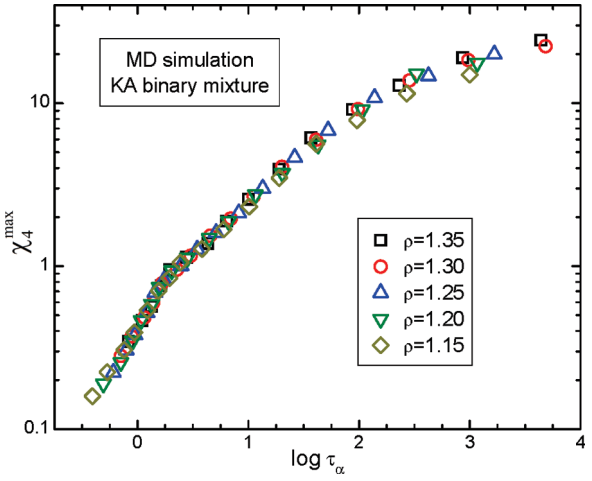

Figure 6. Maximum of the four-point dynamic susceptibility ($= N_c$) as a function of the relaxation time. Each data point represents a different temperature at the density denoted by the symbol type. All quantities are in Lennard-Jones units. Data from ref 112.

correlation function

$$\chi_T(t) = \frac{\partial \Phi(t)}{\partial T} \leq T^{-1}\left(\frac{\Delta c_P}{k_B}\chi_4(t)\right)^{1/2} \tag{9}$$

A lower bound on the number of correlated molecules or segments is obtained as

$$N_c \geq \frac{k_B}{\Delta c_P} T^2 (\chi_T^{max})^2 \tag{10}$$

where χ_T^{max} represents the maximum value of $\chi_T(t)$ for any given state point. Comparisons of simulation results for χ_4 and χ_T indicate a reasonable correspondence between N_c from the two methods,[111] especially near T_g, where to a good approximation the inequality in eq 10 can be replaced by an equal sign.[108,120] The $\chi_T(t)$ approximation has been used to evaluate N_c for different liquids[121,122] and different thermodynamic conditions.[123]

In Figure 7, N_c determined at different temperatures and pressures for four liquids is plotted versus τ_α.[123] For each material N_c is constant to within the experimental uncertainty at any given τ_α. This is the same result seen in the MD simulation (Figure 6), corroborating that the degree of dynamic heterogeneity is determined by the relaxation time. Surprisingly, among different materials, there appears to be a lack of correlation of N_c with either the fragility[118] or β_K.[124]

4. Thermodynamic Scaling of the Dynamics

Time−temperature superpositioning is a popular empirical method of extending the frequency range of experimental data by exploiting the equivalence of time and temperature effects on the dynamics. The superposition principle was derived from free volume concepts, which assume molecular mobility depends on the availability of unoccupied space.[48] Alternatively, dynamic properties can be related to the forces between molecules. This seems especially appropriate in the "jammed" regime near the glass transition, where molecular motions can be interpreted as arising from infrequent, correlated jumps over barriers that are large compared to the thermal energy.[125,126] The complex, multidimensional potential energy landscape governing these intermolecular interactions is commonly approximated by a simple Lennard-Jones (LJ) form,[127] in

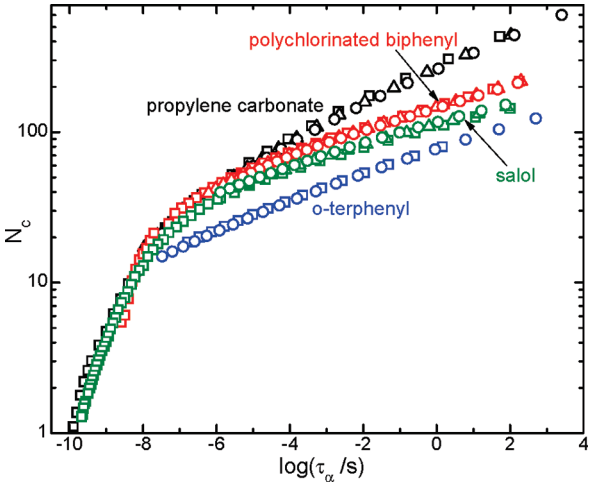

Figure 7. Number of dynamically correlated molecules versus log τ_α, showing that N_c is a material constant at fixed τ_α. For each material different symbols correspond to different pressures, ranging from 0.1 to as much as 500. Data from ref 123.

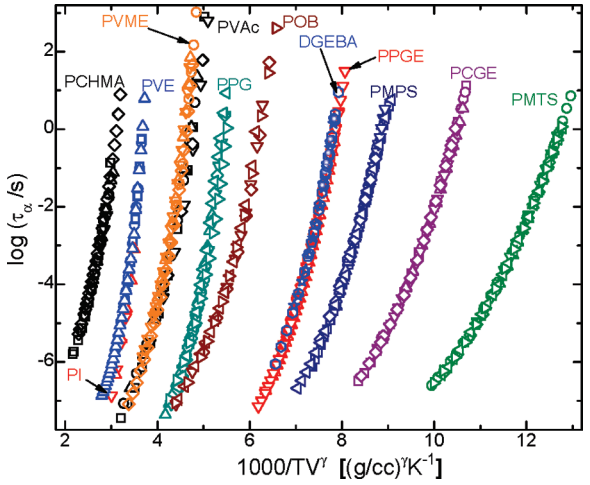

Figure 8. Local segmental relaxation times of polymers versus the product of temperature times the specific volume raised to power of γ = 2.9 (poly(cyclohexyl methacrylate)), 3.0 (polyisoprene), 1.9 (polyvinylethylene), 2.55 (poly(vinyl methyl ether)), 2.6 (poly(vinyl acetate)), 2.5 (poly(propylene glycol)), 2.65 (polyoxybutylene), 2.8 (diglycidyl ether of bisphenol A), 3.5 (poly[(phenyl glycidyl ether)-*co*-formaldehyde]), 5.6 (polymethylphenylsiloxane), 3.3 (poly[(cresylphenyl glycidyl ether)-*co*-formaldehyde]), and 5.0 (polymethytolylsiloxane).

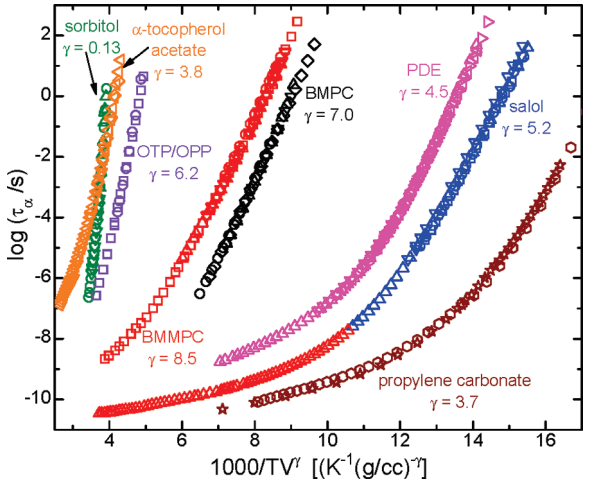

Figure 9. Reorientational relaxation times of supercooled liquids versus the product of temperature times the specific volume raised to the indicated power of γ.

which the potential energy is the sum of independent two-body interactions

$$U(r) = 4\varepsilon_{LJ}[(r_{LJ}/r)^{m_{LJ}} - (r_{LJ}/r)^6] \quad (11)$$

where ε_{LJ}, a microscopic energy, and r_{LJ}, a molecular size, are constants and r is the distance between molecules (LJ particles). For dispersion interactions (no Coulombic forces), the exponent of 6 in the attraction term is universal;[128] however, the steepness of the repulsive interaction, m_{LJ}, varies among materials.[129,130] Since the force on any molecule is the vector sum of the contributions from other molecules, and in condensed matter each molecule (or polymer segment) has many neighbors, attractive forces tend to cancel locally,[131] leading to the classic van der Waals picture, in which the liquid structure is governed by local packing, the attractions exerting only a uniform background pressure.[35,132,133] Accordingly, at least in analyzing local properties, the details of the attractive interactions are sometimes neglected, consistent with the fact that in liquids the static structure factor at intermediate and large wave vectors is sensitive only to the repulsive part of the potential.[134,135]

Dropping the attractive term in eq 11 gives the inverse-power-law (IPL) repulsive potential[136−138]

$$U(r) = [4\varepsilon_{LJ}r_{LJ}^{m_{LJ}}]r^{-m_{LJ}} \quad (12)$$

where the factor in brackets is a constant. If the IPL accurately represents the interaction energy, then thermodynamic properties, such as energy, volume, and entropy, as well as dynamic properties governed by the potential, are a unique function of $r^{m_{LJ}}$ or $V^{m_{LJ}/3}$.[139,140] In practice, not accounting accurately for the attractive forces restricts consideration to local properties; for example, eq 12 does not yield an accurate equation of state.[141,142] An extended version of the IPL potential has been shown to be more broadly applicable.[143]

Neglecting whether the segmental dynamics, having cooperative length scales extending a few nanometers,[116,144−147] can be regarded as sufficiently local to adopt the IPL approximation, the properties of an IPL lead to the expectation that the segmental relaxation times are a function of the variable TV^γ[148−152]

$$\tau_\alpha \sim f(TV^\gamma) \quad (13)$$

where $\gamma \sim m_{LJ}/3$.[153] This scaling of τ_α has been demonstrated for more than 50 materials, both polymers (Figure 8) and small molecules (Figure 9),[19] with γ a material-specific constant. Although eq 13 implies that relaxation involves thermally activated transport over potential barriers, with heights having a volume dependence described by V^γ, semilogarithmic plots of τ_α versus inverse TV^γ are not linear (not Arrhenius). For polymers the magnitude of γ yielding superposition ranges from 1.9 for polyvinylethylene to 5.6 for polymethylphenysiloxane, with values generally smaller than for molecular liquids, for which $3.7 \leq \gamma \leq 8.5$. Smaller γ implies a softer repulsive potential, consistent with a weaker effect of volume (Table 1). Note that[150]

$$E_V/E_P|_{T_g} = (1+\gamma T_g\alpha_P)^{-1} \quad (14)$$

where α_P is the thermal expansion coefficient.

The connection between this TV^γ scaling and the intermolecular potential is substantiated by results from MD simulations. Changing the repulsive exponent alters the effective slope of the repulsive potential, which in turn should change the value of

Table 3. Summary of Parameters from IPL Approximation

m_{LJ}	3γ	effective m_{LJ}[a]	3Γ
8	10.5 ± 0.3	10.9	11.0 ± 0.01
12	15.0 ± 0.3	14.9	15.3 ± 0.01
24	27.3 ± 0.3	27.2	27.2 ± 0.03
36	40.2 ± 0.6	39.9	39.5 ± 0.1

[a] Slope of $U(r)$ over relevant range of interparticle separations.

γ that superposes dynamic data. Simulation results[154] are tabulated in Table 3, where it can be seen that increasing m_{LJ} indeed yields larger γ. However, 3γ is not numerically equal to m_{LJ}; it is always larger. The reason for this is that $U \sim r^{m_{LJ}}$ only in the region of asymptotically small interparticle distances. Over dynamically accessible regions the contribution of the attractive term in eq 11 makes the effective IPL steeper. Included in Table 3 is the exponent of a power-law fit to the potential for values of r between where the radial distribution function first becomes nonzero (i.e., distance of closest approach) and the position of the half-height of its first peak. There is near quantitative correspondence of these effective repulsive slopes with the respective 3γ (Table 3).

For polymers the use of an IPL entails an additional assumption, neglect of contributions from chain stretching and bending modes. Including a harmonic potential for these intrachain motions and using the LJ potential with $m_{LJ} = 12$, Tsolou et al.[155] obtained $\gamma = 2.8$ for the segmental relaxation times of simulated 1,4-polybutadiene; this is *less* than $m/3$. The reason is that the intramolecular degrees of freedom make the repulsive interaction softer,[156] consistent with the smaller experimental values of γ for polymers in comparison to molecular liquids.

Further support for the IPL approximation comes from the fact that for an IPL the virial (structural part of the pressure)

$$W = -\frac{1}{2} r \nabla_r U \tag{15}$$

varies in a simple fashion with the potential[157]

$$\frac{dW}{dU} = \frac{m_{LJ}}{3} \tag{16}$$

This means that for an exact IPL, fluctuations in the viral pressure and the potential energy are perfectly correlated, having a proportionality constant that yields the power law exponent. Results from a number of simulations have shown there is indeed good correlation between U and W (correlation coefficients >0.9) for Lennard-Jones and similar systems;[143,157−159] representative results are shown in Figure 10 for $m_{LJ} = 36$.[159] The ratio $dW/dU \equiv \Gamma$ is equivalent to the value of γ determined from superposing dynamic data; results are listed in Table 3.

5. High-Frequency Dynamics

Dynamic processes transpiring at higher frequency than the α-relaxation precede (in a temporal sense) the glass transition; these include vibrational motions (10^8−10^{13} Hz) and secondary relaxations. The importance of the fast dynamics is that various aspects of the high-frequency behavior correlate with structural relaxation properties, implying that the glass transition begins very much sooner than τ_α. This is the regime addressed by mode-coupling theory.[23−25]

5.1. Johari−Goldstein Secondary Relaxations. Secondary relaxations include trivial movement of some, but not all, atoms in the molecule or repeat unit, examples including motion of a pendant group, chain ends, or atoms in the vicinity of crystal defects. More significant is the Johari−Goldstein (JG) relaxation, which does not involve intramolecular degrees of freedom. The JG relaxation was first

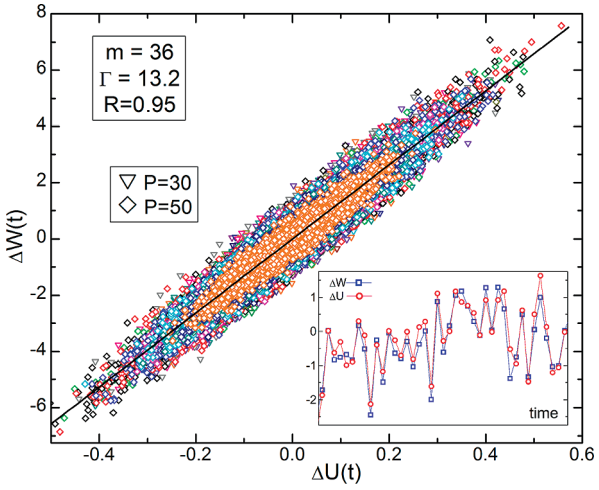

Figure 10. Fluctuations from the mean of the virial plotted against the corresponding fluctuations of the potential energy. Each datum represents a different time at state points corresponding to the indicated pressures (in LJ units) and various temperatures. The straight line is the linear regression, yielding the indicated Γ and correlation coefficient R. The inset shows representative instantaneous fluctuations of the potential energy and virial, both normalized by their respective average values. From ref 159.

discovered in dielectric measurements on rigid molecules[160] and is present in all amorphous or glass-forming materials.[161,162] In small molecules it corresponds to rotation of the entire molecule, although the angle of the reorientation is small, enabling the motion to proceed independently from that of other molecules. For polymers the dynamics of the JG process involves the entire repeat unit. An example is the 180° flip of the pendant carboxyl group in poly(methyl methacrylate) (PMMA), which is coupled to restricted rocking motion of the chain backbone.[163,164] The JG process falls intermediate in time between the caged dynamics and the slower structural relaxation, implying it serves as the precursor of the latter. This follows from the idea that all molecular motions are unconstrained at short times, prior to the buildup of sufficient unbalanced forces and torques from the environment.

The change in the activation energy of the JG relaxation in the vicinity of T_g[79−82] is one indication of a connection to the glass transition.[165,166] Further support is the correlation of various properties:

5.1.1. Relationship between β_K and the Separation of τ_α and τ_{JG}. Since in the glassy state $\tau_{JG}(T)$ has an Arrhenius dependence, an estimate can be obtained for its value at the lowest temperatures at which the α-relaxation is measured. In Figure 11 τ_{JG} is plotted versus β_K for the α-peak determined at T_g for various polymers.[166] There is a correlation between the two quantities, more cooperative structural dynamics (smaller β_K) having greater separation from the noncooperative JG process. In some materials a distinct JG peak is not apparent in relaxation spectra; instead, there is additional intensity on the high-frequency side of the α-dispersion.[167] This "excess wing" phenomenon is observed in materials having narrow α-peaks, in accord with the correlation between τ_{JG} and β_K; that is, an excess wing is just a poorly resolved secondary process due to the small difference between τ_{JG} and τ_α.

According to the coupling model,[166] the identification of the JG process as the noncooperative component of structural relaxation leads to the following prediction

$$\tau_{JG} = {t_c}^{1-\beta_K} {\tau_\alpha}^{\beta_K} \tag{17}$$

in which t_c (~1 ps) is the time at which intermolecular constraints begin to perturb the dynamics. As seen in Figure 11, this

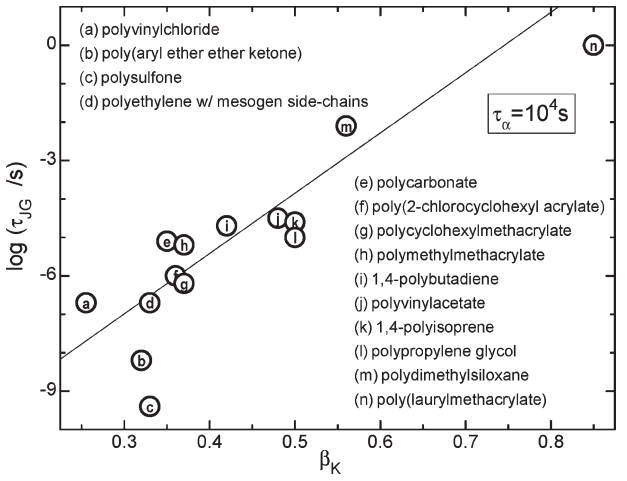

Figure 11. JG relaxation times at T_g (defined as temperature at which $\tau_\alpha = 10^4$ s) as a function of the Kohlrausch exponent for 14 polymers. Equation 17 (solid line), calculated using $t_c = 2 \times 10^{-12}$ s and experimental values for β_K at T_g, has a slope 10% larger than the least-squares linear fit. Data from ref 166.

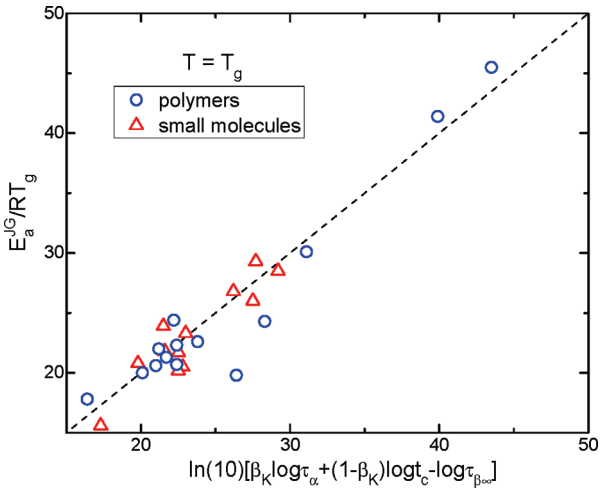

Figure 12. Activation energy for the JG process normalized by RT_g for various polymers and molecular liquids plotted versus the quantity suggested by eq 18 from the coupling model.[172] Pearson correlation coefficient is 0.95; the straight line represents exact equivalence.

equation gives a good accounting for the observed relationship between τ_{JG} and the KWW exponent. Since β_K is constant for a given τ_α (Figure 3), it follows from eq 17 that τ_{JG} is also invariant for such conditions. Thus, for any pressure and temperature that yield the same value of τ_α, τ_{JG} is fixed.[168−170] An example is polyy(phenyl glycidyl ether); for state points from 0.1 MPa and 217 K to 846 MPa and 293 K for which log τ_α (s) = 1, the JG relaxation time remains constant, log τ_{JG} (s) = −5.3 ± 0.3.[170]

5.1.2. Relationship between β_K and JG Activation Energy. Another correlation exists between τ_α and the activation energy for the JG process, E_a^{JG}. Empirically, it was observed that $E_a^{JG} = (24 \pm 3)RT_g$.[171] From eq 17 can be derived the relation[172]

$$E_a^{\beta} = 2.303RT[(\beta_K)\log\tau_\alpha + (1-\beta_K)\log t_c - \log\tau_{\beta\infty}] \quad (18)$$

where $\tau_{\beta\infty}$ is the prefactor in the Arrhenius equation

$$\tau_\beta(T) = \tau_{\beta\infty}\exp(E_a^{JG}/RT) \quad (19)$$

At T_g eq 18 can be written as

$$E_a^{JG}/RT_g = 2.303[-11.7 + 13.7\beta_{KWW} - \log\tau_{\beta\infty}] \quad (20)$$

The two sides of this equation are plotted against one another in Figure 12.[172] Interference from non-JG secondary relaxations limits the availability of data for polymers; therefore, results for molecular liquids are included. There is good correspondence between experimental and calculated values of E_a^{JG}/RT_g, with values scattered around 24, consistent with the empirical observation.[171]

5.1.3. Nonlinear Mechanical Behavior. During mechanical deformation in either the glassy or rubbery states, the elasticity of polymers gives rise to forces perpendicular to the strain direction. For example, shear strain applied through torsion of a cylinder results in a normal force tending to stretch the cylinder. For linear (neo-Hookean) behavior, the ratio of the normal and shear relaxation moduli, $N(t)/G(t)$, is unity.[173] This ratio is plotted in Figure 13[174] for four polymers as a function of time following imposition of a strain equal to ∼4%, which is below the yield point. In each experiment the temperature

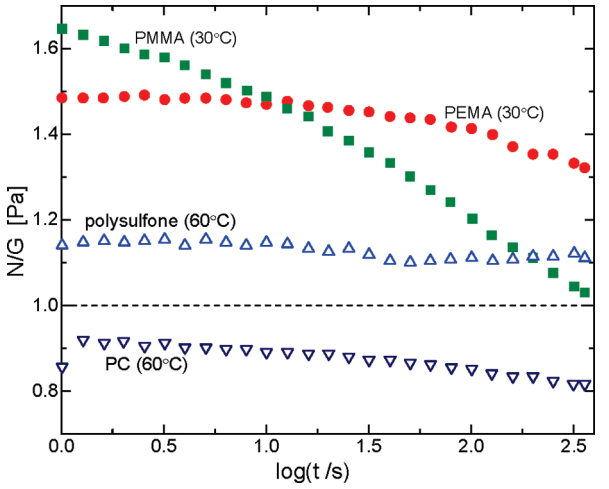

Figure 13. Ratio of the normal force modulus to the torsional modulus for two polymers, PMMA and PEMA, having intense JG relaxations, and two, polysulfone and PC, having weak, main-chain secondary relaxations. The former exhibit strong deviations from neo-Hookean behavior (indicated by the horizontal dashed line). The measurements were done at the respective peak temperatures of the secondary relaxation. From ref 174.

(< T_g) corresponds to the peak in the mechanical spectrum due to the secondary relaxation. Two materials, PMMA and poly(ethyl methacrylate) (PEMA), have intense secondary relaxations that, although arising primarily from side groups, are cooperative with the chain and thus JG-type processees.[166] The mechanical response of these polymethacrylates is strongly nonlinear, $N(t)/G(t) \sim 1.5$ at shorter times. The other two polymers, polysulfone and polycarbonate (PC), have weak JG relaxations associated with low-amplitude backbone motions, and their behavior is nearly linear ($N(t)/G(t)$ within about 10% of unity). The implication is that the JG relaxation governs the normal force and associated deviations from neo-Hookean behavior.[174] This is not an obvious result, since the chain displacement necessary to accommodate a 4% strain exceeds the amplitude of the local JG motion, involving dimensions on the order of 10 nm.[175]

5.2. Caged Dynamics. Short-ranged repulsive forces give rise to high-frequency oscillations, which have an amplitude quantified by the mean-square displacement, $\langle r^2 \rangle$. Escape of

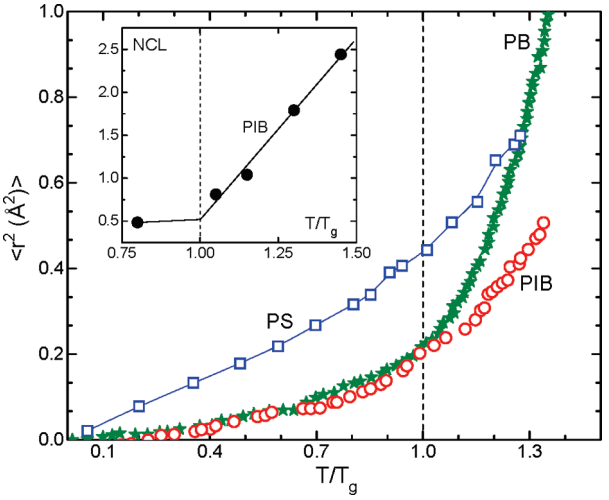

Figure 14. Variation of the mean-squared displacement with temperature, showing the change in T dependence around T_g, for polystyrene,[178] 1,4-polybutadiene,[179] and polyisobutylene.[180] The inset shows the corresponding behavior of the nearly constant loss in PIB.[184]

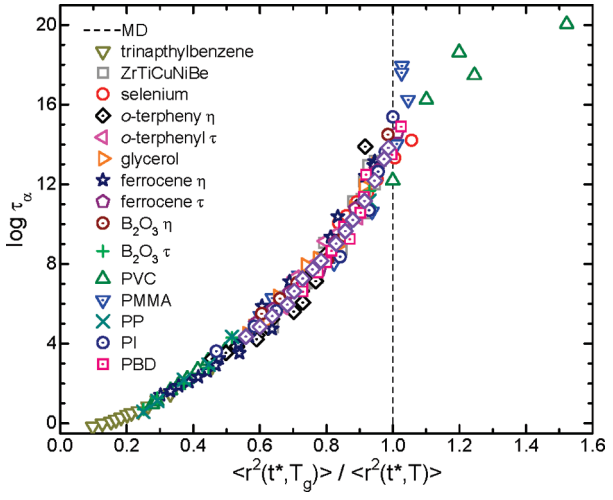

Figure 15. Structural relaxation times (MD units) versus the inverse of the mean-square displacement normalized by the value at T_g for various glass-forming materials, including poly(vinyl chloride), poly(methyl methacrylate), polypropylene, 1,4-polyisoprene, and 1,4-polybutadiene. The data for each material correspond to different temperatures, with $\langle r^2 \rangle$ evaluated at the time, t^*, corresponding to the minimum in the velocity correlation function, which is at least an order of magnitude shorter than τ_α. The glass transition is denoted by the vertical dashed line. From ref 185.

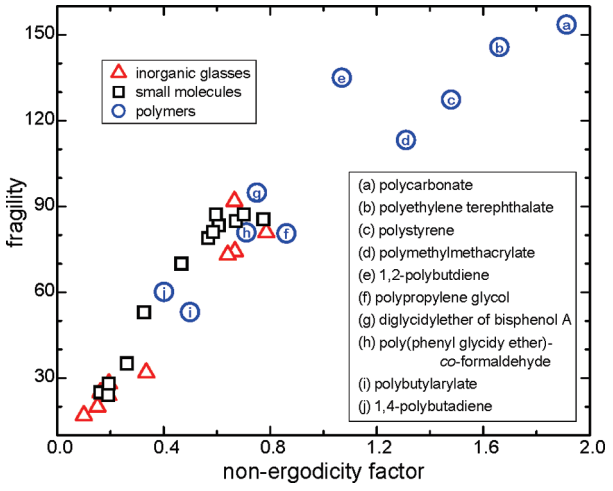

Figure 16. Fragility of various glass-forming materials versus the nonergodicity parameter (long time plateau in the Debye−Waller factor = $\exp(-\langle r^2 \rangle q^2/2)$, where q is the scattering vector, measured in the glassy state). From ref 187.

molecules or polymer segments from their nearest-neighbor cages makes an additional contribution to $\langle r^2 \rangle$, referred to as the fast relaxation and manifested in scattering experiments as a nearly constant loss; that is, a broad minimum in the dynamic susceptibility observed at gigahertz frequencies near T_g or lower frequencies far below T_g.[176,177] This fast relaxation occurs at much shorter times than the reorientations and diffusions that dissolve the local liquid structure and give rise to the glass−liquid transition. However, despite the disparity in time scales, the microscopic mean-square displacement changes temperature dependence near T_g.[22,178−183] This is illustrated for three polymers in Figure 14; $\langle r^2 \rangle$ rises more steeply above T_g, implying that the fast dynamics sense structural relaxation. Similarly, the magnitude of the nearly constant loss changes behavior at T_g (Figure 14, inset[184]). And strikingly, there is an almost universal dependence of $\langle r^2 \rangle$ on τ_α when the former is measured at times much shorter than τ_α, as shown in Figure 15 for five polymers and several molecular liquids.[185]

Other experimental results indicating a connection between the short time and the structural dynamics include the correlation of $\langle r^2 \rangle$ at T_g with β_K[178] and the correlation of the fragility with the plateau value of $\langle r^2 \rangle$ measured in the glassy state (Figure 16)[186,187] and with the power law exponent describing the change with pressure in the ratio of the transverse Brillouin and Boson peak frequencies (Figure 17).[188] This ratio is related to a characteristic length scale of the glassy state.[189,190] The relevant point is that a property obtained from measurement of vibrational motions at frequencies in the range 10^9-10^{12} Hz can be connected to the (many orders of magnitude) slower α-relaxation.

6. Aging and Relaxation in the Glassy State

Usually studies of the glass transition do not investigate the glassy state *per se*; rather, the focus is on the behavior of the equilibrium material when vitrification is imminent and τ_α increases in non-Arrhenius fashion. Below T_g τ_α becomes too large for direct measurement, but an obvious inquiry is what happens to τ_α in the glass. This is important because without any change in T dependence τ_α would diverge at T_V. If τ_α is governed by the configurational entropy,[97] this implies a violation of the third law of thermodynamics upon cooling below T_V.[191] A related issue concerns the putative existence of an ideal glass transition, that is, a thermodynamic phase change rather than the kinetic phenomenon actually observed.[32,33] Experiments indicate that such an ideal glass transition is nonexistent,[34−37] the Kauzmann paradox avoided because the non-Arrhenius temperature dependence above T_g becomes weaker, Arrhenius behavior in the glass.[38,39,192−194]

Since a glass is out of equilibrium, properties such as volume, enthalpy, and entropy all decrease over time at a rate that decreases with the extent of cooling. This phenomenon, known as physical aging, becomes immeasurably slow well below T_g. However, recently Ediger and co-workers[195,196] discovered a means to achieve a glassy state having unusually low enthalpy and high density, corresponding to aging times of many millennia. This is accomplished by slow vapor deposition below T_g (a method inapplicable to polymers). The mechanism appears to be the enhanced mobility of each surface layer, allowing close approach to equilibrium prior to arrival of subsequent layers.

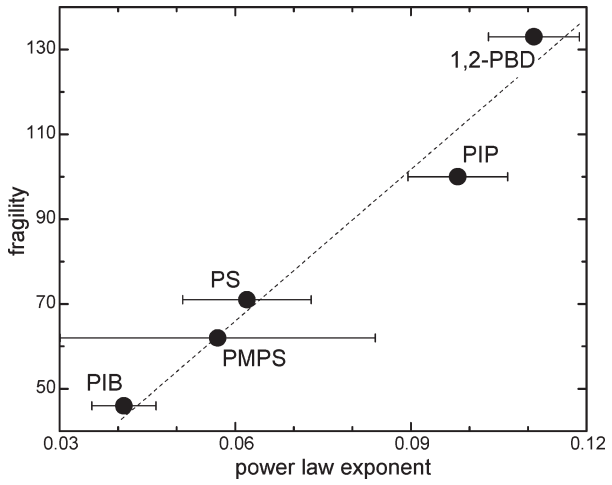

Figure 17. Fragility of five polymers versus the exponent, X, of the pressure dependence of the ratio of transverse Brillioun and Boson peak frequencies, $\nu_{TA}/\nu_{BP} \sim P^{-X}$. From ref 188.

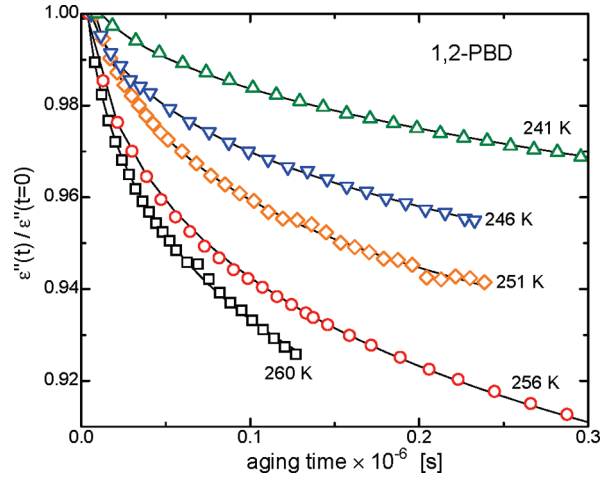

Figure 18. Dielectric loss at 1 kHz versus aging time for polyvinylethylene at five temperatures below T_g (=272 K). The ordinate values are normalized to the initial value. The solid line is the fit to KWW function eq 2 with t taken as the aging time. The KWW time constant for physical aging increases with decrease of the aging temperature. The longest value deduced for τ_α is about 1 year, which is 100-fold longer than the time of the measurements. From ref 193.

Physical aging affects many properties, including the relaxation times and the dielectric strength of the JG process.[193,194,197−199] This is illustrated for polyvinylethylene in Figure 18, where the shift of the JG relaxation to higher frequencies causes a decrease in the dielectric loss at frequencies on the low side of the JG peak. The evolution of the JG properties in the glassy state reflects the aging dynamics, so that the time constant for these changes provides a measure of τ_α, which cannot be obtained by conventional techniques. Figure 19[193,194] shows τ_α for two polymers, directly measured above T_g and deduced for the glassy state from the kinetics of the change in the JG relaxation. Also shown are similar data obtained by measuring the reorientational motion of a chromophore embedded in a polystyrene.[192] These results all confirm the change in T dependence of τ_α, with the behavior becoming Arrhenius in the glassy state.

Mechanical deformation of a glassy polymer usual entails substantial chain displacements, involving multiple backbone conformational transitions;[200] thus, there is a connection between the mechanical response of a glass and local chain mobility.[201,202] This is seen in classic "tickle" experiments, in which a small strain

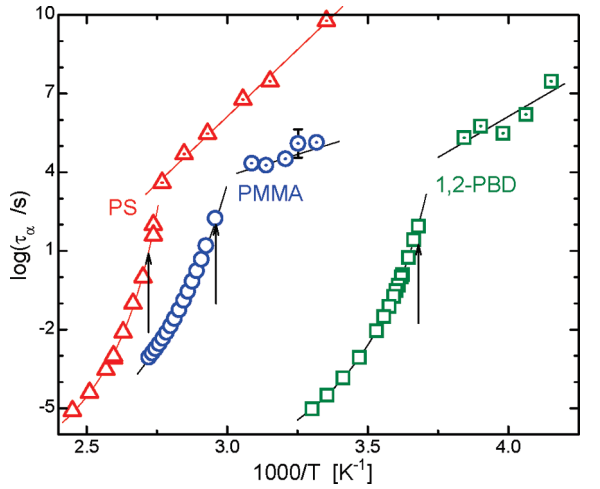

Figure 19. Segmental relaxation times measured above T_g (open symbols) and in the glassy state (dotted symbols) for polystyrene (triangles),[192] poly(methyl methacrylate) (circles),[194] and polyvinylethylene (squares).[193] The non-Arrhenius behavior is absent below T_g (denoted by the arrows).

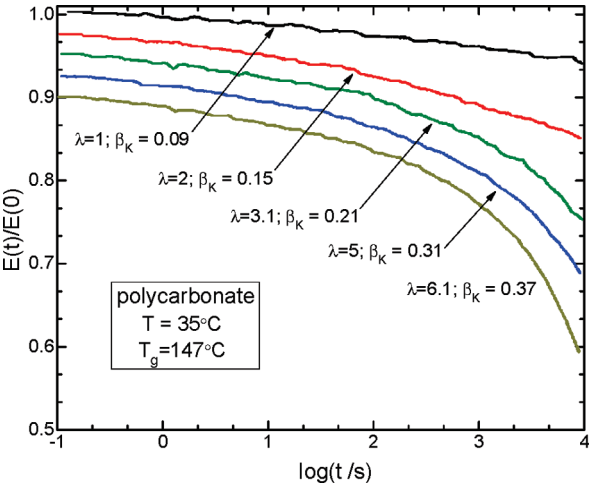

Figure 20. Tensile stress relaxation modulus measured following imposition of a 0.2% strain in glassy polycarbonate deformed to the indicated stretch ratios, λ. With increasing deformation, the relaxation of the small perturbation is faster and associated with decreasing nonexponentiality, as indicated by the values of the KWW exponent. The curves were normalized by the moduli at 0.1 s and shifted vertically for clarity. From ref 204.

is applied subsequent to imposition of a much larger strain.[203] In Figure 20,[204] small-strain stress relaxation curves are shown for glassy polycarbonate. The decay is faster and associated with a larger β_K as the large tensile strain is increased. More recent experiments, using optical probes that are not coupled to the primary deformation, confirm this enhanced mobility (Figure 21[205]). Such experiments suggest that the constraints on the local dynamics are affected by mechanical strain, analogous to the restricted configurational freedom of network chains in cross-linked rubbery polymers.[206] The latter is the operative mechanism in constraint models of rubber elasticity.[207]

7. Confinement Effects

When a material is constrained to a sufficient extent (spatial dimension h < 100 nm), its glass transition temperature often becomes lower than T_g of the bulk state.[208,209] This effect is well-established for free-standing films (Figure 22[209]) and often is found for supported films and material confined within nanopores,[210−212]

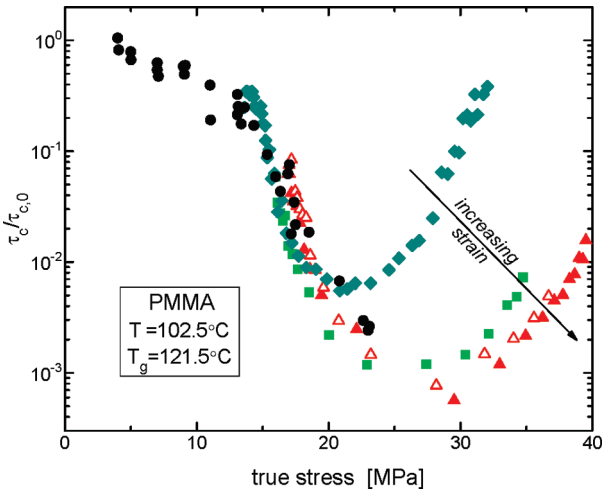

Figure 21. Reorientational correlation time of a probe molecule versus true stress during creep of PMMA. Different curves correspond to engineering stresses in the range 13.5−16.0 MPa. Prior to the onset of strain hardening, the local mobility increases with tensile strain. The ordinate values were normalized by the correlation time measured in the absence of strain. From ref 205.

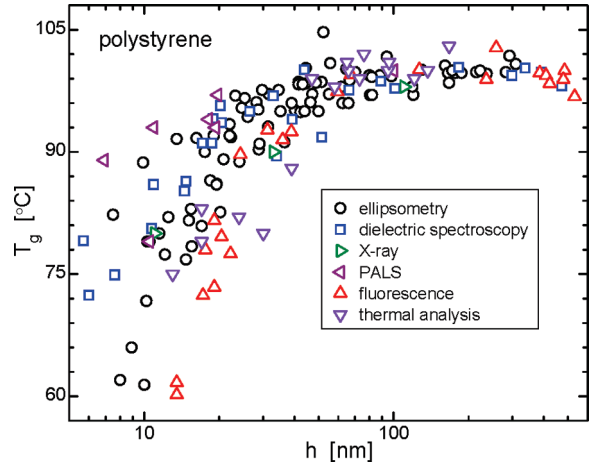

Figure 22. Glass transition temperature as a function of the thickness of free-standing films of atactic PS measured by the indicated methods.[209] The variation of M_w among samples causes some of the spread of the data, given the molecular weight dependence of $T_g(h)$.

although the effect may be weaker for the latter conditions due to substrate interaction.[213−215] The mechanism for the T_g reduction in confined materials seems to be the enhanced mobility of surface molecules,[216−221] a result of fewer constraints from neighbors and/or greater unoccupied volume. However, this explanation alone cannot account for many details of the phenomenon. Experiments reveal a molecular weight dependence, as shown in Figure 23 for PS[222] and PMMA,[223] although for molecular weights less than ca. 400 kg/mol, the $T_g(h)$ behavior appears to become invariant to molecular weight[222] (Figure 24). The effect of confinement also varies with chemical structure; for example, PS is more sensitive than PMMA (Figure 23), which in turn has greater sensitivity to h than other acrylate polymers.[224] A change in tacticity in PMMA can change qualitatively the effect of film thickness on T_g[225,226] (Figure 25), though such results are for supported films, where the possibility exists for complications from the substrate.

Similar reductions in T_g result from the morphology of phase-segregated block copolymers, although of less magnitude than for free-standing films (Figure 24[227,228]). Filler particles also can enhance segmental mobility,[225,229−232] provided there is no

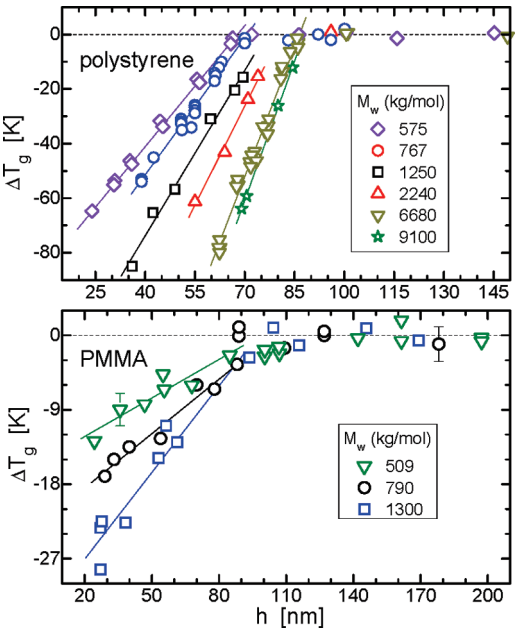

Figure 23. Effect of molecular weight on confinement dependence T_g for free-standing films of PS[222] and PMMA.[223] The polymers are primarily atactic, although the PMMA had small tacticity differences and consequent small differences in the bulk values of T_g.

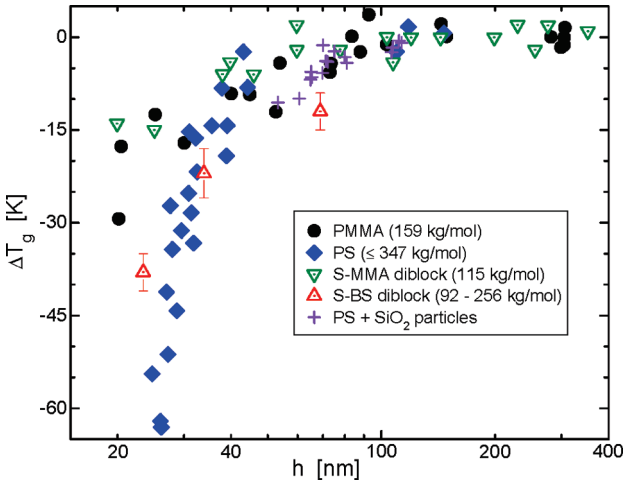

Figure 24. Confinement-induced changes in glass transition temperature of PMMA (filled circles[223]) and various lower M_w PS homopolymers (filled diamonds[222]), along with data for the styrene block in diblock copolymers with methyl methacrylate (open inverted triangles[227]) and random butadiene−styrene (open triangles[228]). Molecular weights are indicated for the homopolymers or the styrene block for the copolymers. Also shown are T_g of bulk PS homopolymer (crosses[229]) containing various concentrations of silica nanoparticles.

adsorption at the filler surface.[233,234] Some results are shown in Figures 24 and 25, where h is the distance between particles. Note that quantitative correspondence between film thickness and particle separation requires judicious selection of the average value used for h.[235] The T_g depression is more significant for fillers with softer surfaces.[228,236] Traditional carbon black and silica fillers generally have too large a particle size for measurable changes in T_g.[233,237]

The effect of confinement on the dynamics of polymers and more generally of supercooled liquids requires better understanding, but this is complicated by the many anomalies. Different experimental methods can yield different or negligible h dependences.[238−243] Many experimentalists employ dielectric spectroscopy, but the

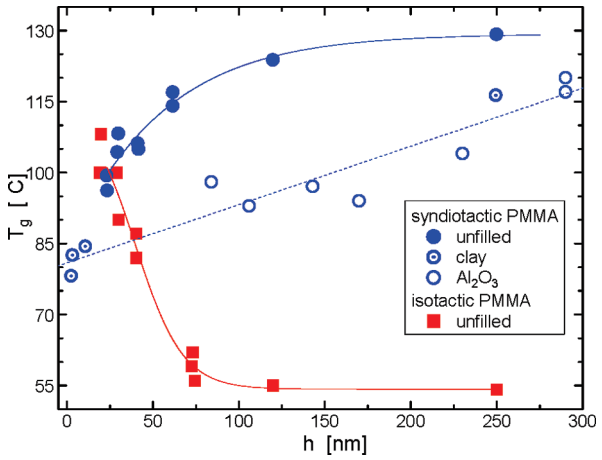

Figure 25. Variation of T_g with thickness for different stereoregular PMMA films on silicon substrates (solid symbols).[225] Results are also shown for syndiotactic PMMA containing various concentrations of bentonite clay (dotted circles)[225] or alumina particles (open circles).[230] For the neat PMMA h is the film thickness; for filled PMMA h represents a mean distance between particles.

measured permittivity is not additive in the layer contributions, so that dielectrically inactive regions at the electrode surface can shift the relaxation peak without any actual change in the dynamics.[244] When T_g is reduced in thin films, quantities presumably associated with greater segmental mobility above T_g, such as the heat capacity,[242,245] thermal expansivity,[224,246] and chain diffusivity,[247] may be reduced.

8. Summary

A complete theory of the glass transition must address a wide range of experimental results. Those described herein include the following:

(i) Temperature and volume have a near-equivalent effect on the magnitude of τ_α near T_g.

(ii) For a fixed value of τ_α, the shape of the relaxation dispersion, the number dynamically correlated molecules, the JG-relaxation time, and the product variable TV^γ are all constant, independent of T, P, and V.

(iii) Although the temperature of the dynamic crossover changes with pressure, the relaxation time at T_B is a material constant.

(iv) Relaxation processes transpiring at high frequencies, and thus usually only measured in the glassy state, are correlated in various ways with structural relaxation properties of the equilibrium liquid, implying that the short time dynamics anticipate the glass transition. This effect is most apparent for the JG relaxation, implying that it serves as the precursor of structural relaxation.

(v) Spatial confinement often reduces T_g and increases local mobility; however, the phenomenon depends on the nature of the confining surface, the chemical structure and even tacticity of the material, and its molecular weight.

Acknowledgment. This work was supported by the Office of Naval Research. Stimulating discussions with K. L. Ngai and C. G. Robertson are gratefully acknowledged. The author thanks J. R. Dutcher, M. D. Ediger, D. Leporini, K. L. Ngai, and C. G. Robertson for kindly providing their data.

References and Notes

(1) Einstein, A. In *Investigations on the Theory of the Brownian Movement*; Fuerth, R., Ed., Cowper, A. D., Translator; Methuen Co.: London, 1926; Dover Publ.: New York, 1956.
(2) Debye, P. *Polar Molecules*; Dover: New York, 1928.
(3) Persson, B. N. J. *Surf. Sci.* **1998**, *401*, 445.
(4) Kluppel, M.; Heinrich, G. *Rubber Chem. Technol.* **2000**, *73*, 578.
(5) Persson, B. N. J.; Tartaglino, U.; Albohr, O.; Tosatti, E. *Phys. Rev. B* **2005**, *71*, 035428.
(6) Bond, R.; Morton, G. F.; Krol, L. H. *Polymer* **1984**, *25*, 132.
(7) Rahalkar, R. R. *Rubber Chem. Technol.* **1989**, *62*, 246.
(8) Takino, H.; Nakayama, R.; Yamada, Y.; Kohjiya, S.; Matsuo, T. *Rubber Chem. Technol.* **1997**, *70*, 584.
(9) Heinrich, G.; Dumler, H. B. *Rubber Chem. Technol.* **1998**, *71*, 53.
(10) Barsoum, R. G. S.; Dudt, P. J. *AMMTIAC Q.* **2010**, *4* (4), 11.
(11) Bogoslovov, R.; Roland, C. M.; Gamache, R. M. *Appl. Phys. Lett.* **2007**, *90*, 221910.
(12) Roland, C. M.; Fragiadakis, D.; Gamache, R. M. *Compos. Struct.* **2010**, *92*, 1059.
(13) *Sound and Vibration Damping with Polymers*; Corsaro, R. D., Sperling, L. H., Eds.; ACS Symposium Series 424; American Chemical Society: Washington, DC, 1990.
(14) Gosline, J. M. *Rubber Chem. Technol.* **1987**, *60*, 417.
(15) Cavagna, A. *Phys. Rep.* **2009**, *476*, 51.
(16) Chen, K.; Saltzman, E. J.; Schweizer, K. S. *J. Phys.: Condens. Matter* **2009**, *21*, 503101.
(17) Kivelson, S. A.; Tarjus, G. *Nature Mater.* **2008**, *7*, 831.
(18) Dyre, J. C. *Rev. Mod. Phys.* **2006**, *78*, 953.
(19) Roland, C. M.; Hensel-Bielowka, S.; Paluch, M.; Casalini, R. *Rep. Prog. Phys.* **2005**, *68*, 1405.
(20) Debenedetti, P. G.; Stillinger, F. H. *Nature* **2001**, *410*, 259.
(21) Lunkenheimer, P. *Contemp. Phys.* **2000**, *41*, 15.
(22) Angell, C. A.; Ngai, K. L.; McKenna, G. B.; McMillan, P. F.; Martin, S. W. *J. Appl. Phys.* **2000**, *88*, 3113.
(23) Gotze, W. J. *Complex Dynamics of Glass-Forming Liquids*; Oxford University Press: Oxford, UK, 2009.
(24) Gotze, W. *J. Phys.: Condens. Matter* **1999**, *11*, A1.
(25) Reichman, D. R.; Charbonneau, P. *J. Stat. Mech.* **2005**, P05013.
(26) Tracht, U.; Heuer, A.; Reinsberg, S. A.; Spiess, H. W. *Appl. Magn. Reson.* **1999**, *17*, 227.
(27) Helfand, E. *Science* **1984**, *226*, 647.
(28) Bahar, I.; Erman, B.; Monnerie, L. *Macromolecules* **1991**, *24*, 3618.
(29) Tanaka, H.; Kawasaki, T.; Shintani, H.; Watanabe, K. *Nature Mater.* **2010**, *9*, 324.
(30) Roland, C. M.; Ngai, K. L.; Santangelo, P. G.; Qiu, X. H.; Ediger, M. D.; Plazek, D. J. *Macromolecules* **2001**, *34*, 6159.
(31) (a) Vogel, H. *Phys. Z.* **1921**, *22*, 645. (b) Fulcher, G. S. *J. Am. Ceram. Soc.* **1925**, *8*, 339. (c) Tammann, G.; Hesse, W. *Z. Anorg. Allg. Chem.* **1926**, *156*, 245.
(32) Debenedetti, P. G. *Metastable Liquids: Concepts and Principles*; Princeton University Press: Princeton, NJ, 1996.
(33) Donth, E. *The Glass Transition: Relaxation Dynamics in Liquids and Disordered Materials*; Springer: New York, 2001.
(34) Simon, S. L.; McKenna, G. B. *J. Non-Cryst. Solids* **2009**, *355*, 672.
(35) Stillinger, H.; Debenedetti, P. G.; Truskett, T. M. *J. Phys. Chem. B* **2001**, *105*, 11809.
(36) Hecksher, T.; Nielsen, A. I.; Olsen, N. B.; Dyre, J. C. *Nature Phys.* **2008**, *4*, 737.
(37) Donev, A.; Stillinger, F. H.; Torquato, S. *Phys. Rev. Lett.* **2006**, *96*, 225502.
(38) O'Connell, P. A.; McKenna, G. B. *J. Chem. Phys.* **1999**, *110*, 11054.
(39) Simon, S. L.; Sobieski, J. W.; Plazek, D. J. *Polymer* **2001**, *42*, 2555.
(40) Chamberlin, R. V. *Phys. Rev. Lett.* **1999**, *82*, 2520.
(41) Casalini, R.; Mohanty, U.; Roland, C. M. *J. Chem. Phys.* **2006**, *125*, 014505.
(42) Mauro, J. C.; Yue, Y.; Ellison, A. J.; Gupta, P. K.; Allan, D. C. *Proc. Natl. Acad. Sci. U.S.A.* **2009**, *106*, 19780.
(43) Angell, C. A. *J. Non-Cryst. Solids* **1991**, *131*, 13.
(44) Plazek, D. J. *J. Rheol.* **1996**, *40*, 987.
(45) Ngai, K. L.; Plazek, D. J. *Rubber Chem. Technol.* **1995**, *68*, 376.
(46) Santangelo, P. G.; Roland, C. M. *Macromolecules* **1998**, *31*, 3715.
(47) Sokolov, A. P.; Schweizer, K. S. *Phys. Rev. Lett.* **2009**, *102*, 248301.
(48) Ferry, J. D. *Viscoelastic Properties of Polymers*, 3rd ed.; Wiley: New York, 1980.
(49) Doi, M.; Edwards, S. F. *The Theory of Polymer Dynamics*; Clarendon Press: Oxford, 1986.
(50) McLeish, T. C. B. *Adv. Phys.* **2002**, *51*, 1379.
(51) Ding, Y.; Sokolov, A. P. *Macromolecules* **2006**, *39*, 3322.

(52) Ngai, K. L.; Plazek, D. J.; Roland, C. M. *Macromolecules* **2006**, *39*, 3322.
(53) Grest, G. S.; Cohen, M. H. *Adv. Chem. Phys.* **1981**, *48*, 455.
(54) Miyamoto, T.; Shibayama, K. *J. Appl. Phys.* **1973**, *44*, 5372.
(55) Naoki, M.; Endou, H.; Matsumoto, K. *J. Phys. Chem.* **1987**, *91*, 4169.
(56) Williams, G. In *Dielectric Spectroscopy of Polymeric Materials*; Runt, J. P., Fitzgerald, J. J., Eds.; American Chemical Society: Washington, DC, 1997.
(57) Casalini, R.; Roland, C. M.; Capaccioli, S. *J. Chem. Phys.* **2007**, *126*, 184903.
(58) Casalini, R.; Roland, C. M. *J. Chem. Phys.* **2003**, *119*, 11951.
(59) Santangelo, P. G., unpublished results.
(60) Casalini, R.; Ngai, K. L.; Roland, C. M. *Phys. Rev. B* **2003**, *68*, 014201.
(61) Stickel, F.; Fischer, E. W.; Richert, R. *J. Chem. Phys.* **1995**, *102*, 6251; **1996**, *104*, 2043.
(62) Ngai, K. L.; Roland, C. M. *Polymer* **2002**, *43*, 567.
(63) Colmenero, J.; Alegria, A.; Santangelo, P. G.; Ngai, K. L.; Roland, C. M. *Macromolecules* **1994**, *27*, 407.
(64) Cangialosi, D.; Alegría, A.; Colmenero, M. *J. Chem. Phys.* **2009**, *130*, 124902.
(65) Richert, R. *J. Chem. Phys.* **2005**, *123*, 154502.
(66) Richert, R.; Duvvuri, K.; Duong, L.-T. *J. Chem. Phys.* **2003**, *118*, 1828.
(67) Rajian, J. R.; Huang, W.; Richert, R.; Quitevis, E. L. *J. Chem. Phys.* **2006**, *124*, 014510.
(68) Bogoslovov, R. B.; Hogan, T. E.; Roland, C. M. *Macromolecules* **2010**, *43*, 2904.
(69) (a) Kohlrausch, R. *Ann. Phys. Chem.* (*Poggendorff*) **1854**, *91*, 179. (b) Williams, G.; Watts, D. C. *Trans. Faraday Soc.* **1970**, *66*, 80.
(70) Roland, C. M.; Casalini, R. *J. Non-Cryst. Solids* **2007**, *353*, 3996.
(71) Analytical expressions for the KWW equation and other susceptibility functions are given in: Hilfer, R. *Phys. Rev. E* **2002**, *65*, 061510.
(72) Roland, C. M.; Casalini, R.; Paluch, M. *Chem. Phys. Lett.* **2003**, *367*, 259.
(73) Ngai, K. L.; Casalini, R.; Capaccioli, S.; Paluch, M.; Roland, C. M. *J. Phys. Chem. B* **2005**, *109*, 17356.
(74) Ngai, K. L.; Casalini, R.; Capaccioli, S.; Paluch, M.; Roland, C. M. In *Advances in Chemical Physics*; Kalmykov, Y. P., Coffey, W. T., Rice, S. A., Eds.; Wiley: New York; 2006, Vol. *133B*, Chapter 10.
(75) Ngai, K. L.; Roland, C. M. *Polymer* **2002**, *43*, 567.
(76) Stickel, F.; Fischer, E. W.; Richert, R. *J. Chem. Phys.* **1996**, *104*, 2043.
(77) Schulz, M.; Donth, E. *J. Non-Cryst. Solids* **1994**, *168*, 186.
(78) Rault, J. *J. Non-Cryst. Solids* **2000**, *271*, 177.
(79) Wagner, H.; Richert, R. *J. Phys. Chem. B* **1999**, *103*, 4071.
(80) Fujima, T.; Frusawa, H.; Ito, K. *Phys. Rev. E* **2002**, *66*, 031503.
(81) Nozaki, R.; Zenitani, H.; Minoguchi, A.; Kitai, K. *J. Non-Cryst. Solids* **2002**, *307*−*310*, 349.
(82) Paluch, M.; Roland, C. M.; Pawlus, S.; Ziolo, J.; Ngai, K. L. *Phys. Rev. Lett.* **2003**, *91*, 115701.
(83) Ediger, M. D.; Angell, C. A.; Nagel, S. R. *J. Phys. Chem.* **1996**, *100*, 13200.
(84) Ngai, K. L.; Magill, J. H.; Plazek, D. J. *J. Chem. Phys.* **2000**, *112*, 1887.
(85) Chang, I.; Sillescu, H. *J. Phys. Chem. B* **1997**, *101*, 8794.
(86) Comez, L.; Fioretto, D.; Palmieri, L.; Verdini, L.; Rolla, P. A.; Gapinski, J.; Pakula, T.; Patkowski, A.; Steffen, W.; Fischer, E. W. *Phys. Rev. E* **1999**, *60*, 3086.
(87) Corezzi, S.; Campani, E.; Rolla, P. A.; Capaccioli, S.; Fioretto, D. *J. Chem. Phys.* **1999**, *111*, 9343.
(88) Casalini, R.; Roland, C. M. *J. Chem. Phys.* **2003**, *119*, 4052.
(89) Hall, D. B.; Deppe, D. D.; Hamilton, K. E.; Dhinojwala, A.; Torkelson, J. M. *J. Non-Cryst. Solids* **1998**, *235*, 48.
(90) Faetti, M.; Giordano, M.; Leporini, D.; Pardi, L. *Macromolecules* **1999**, *32*, 1876.
(91) Casalini, R.; Paluch, M.; Roland, C. M. *J. Chem. Phys.* **2003**, *118*, 5701.
(92) Casalini, R.; Roland, C. M. *Phys. Rev. Lett.* **2004**, *92*, 245702.
(93) Bair, S.; Roland, C. M.; Casalini, R. *Proc. Inst. Mech. Eng., Part J* **2007**, *221*, 801.
(94) Roland, C. M.; Casalini, R. *J. Non-Cryst. Solids* **2005**, *351*, 2581.
(95) Casalini, R.; Roland, C. M. *Phys. Rev. B* **2005**, *71*, 014210.
(96) Novikov, V. N.; Sokolov, A. P. *Phys. Rev. E* **2003**, *67*, 031507.
(97) Adam, G.; Gibbs, J. H. *J. Chem. Phys.* **1965**, *43*, 139.
(98) Biroli, G.; Bouchaud, J.-P.; Miyazaki, K.; Reichman, D. R. *Phys. Rev. Lett.* **2006**, *97*, 195701.
(99) Sillescu, H. *J. Non-Cryst. Solids* **1999**, *243*, 81.
(100) Tarjus, G.; Kivelson, S. A.; Nussinov, Z.; Viot, P. *J. Phys.: Condens. Matter* **2005**, *17*, R1143.
(101) (a) Lubchenko, V.; Wolynes, P. G. *Annu. Rev. Phys. Chem.* **2007**, *58*, 235. (b) Xia, X. Y.; Wolynes, P. G. *Proc. Natl. Acad. Sci. U.S.A.* **2000**, *97*, 2990.
(102) Avramov, I. *J. Non-Cryst. Solids* **2005**, *351*, 3163.
(103) Franz, S.; Parisi, G. *J. Phys.: Condens. Matter* **2000**, *12*, 6335.
(104) Chandler, D.; Garrahan, J. P.; Jack, R. L.; Maibaum, L.; Pan, A. C. *Phys. Rev. E* **2006**, *74*, 051501.
(105) Fischer, E. W.; Donth, E.; Steffen, W. *Phys. Rev. Lett.* **1992**, *68*, 2344.
(106) Bohmer, R.; Chamberlin, R. V.; Diezemann, G.; Geil, B.; Heuer, A.; Hinze, G.; Kuebler, S. C.; Richert, R.; Schiener, B.; Sillescu, H.; Spiess, H. W.; Tracht, U.; Wilhelm, M. *J. Non-Cryst. Solids* **1998**, *235*−*237*, 1.
(107) Franz, S.; Donati, C.; Parisi, G.; Glotzer, S. C. *Philos. Mag. B* **1999**, *79*, 1827.
(108) Dalle-Ferrier, C.; Thibierge, C.; Alba-Simionesco, C.; Berthier, L.; Biroli, G.; Bouchaud, J. P.; Ladieu, F.; L'Hote, D.; Tarjus, G. *Phys. Rev. E* **2007**, *76*, 041510.
(109) Vollmayr-Lee, K.; Kob, W.; Binder, K.; Zippelius, A. *J. Chem. Phys.* **2002**, *116*, 5158.
(110) Lacevic, N.; Starr, F. W.; Schrøder, T. B.; Glotzer, S. C. *J. Chem. Phys.* **2003**, *119*, 7372.
(111) Berthier, L.; Biroli, G.; Bouchaud, J.-P.; Kob, W.; Miyazaki, K.; Reichman, D. R. *J. Chem. Phys.* **2007**, *126*, 184503.
(112) Coslovich, D.; Roland, C. M. *J. Chem. Phys.* **2009**, *131*, 151103.
(113) Schmidt-Rohr, K.; Spiess, H. W. *Phys. Rev. Lett.* **1991**, *66*, 3020.
(114) Cicerone, M. T.; Blackburn, F. R.; Ediger, M. D. *Macromolecules* **1995**, *28*, 8224.
(115) Donth, E. *J. Non-Cryst. Solids* **1982**, *53*, 325.
(116) Hempel, E.; Hempel, G.; Hensel, A.; Schick, C.; Donth, E. *J. Phys. Chem. B* **2000**, *104*, 2460.
(117) Kremer, F.; Huwe, A.; Arndt, M.; Behrens, P.; Schwieger, W. *J. Phys.: Condens. Matter* **1999**, *11*, A175.
(118) Hong, L.; Gujrati, P. D.; Novikov, V. N.; Sokolov, A. P. *J. Chem. Phys.* **2009**, *131*, 194511.
(119) Berthier, L.; Biroli, G.; Bouchaud, J.-P.; Cipelletti, L.; El Masri, D.; L'Hôte, D.; Ladieu, F.; Pierno, M. *Science* **2005**, *310*, 1797.
(120) Berthier, L.; Biroli, G.; Bouchaud, J. P.; Kob, W.; Miyazaki, K.; Reichman, D. *J. Chem. Phys.* **2007**, *126*, 184504.
(121) Dalle-Ferrier, C.; Eibl, S.; Pappas, C.; Alba-Simionesco, C. *J. Phys.: Condens. Matter* **2008**, *20*, 494240.
(122) Capaccioli, S.; Ruocco, G.; Zamponi, F. *J. Phys. Chem. B* **2008**, *112*, 10652.
(123) Fragiadakis, D.; Casalini, R.; Roland, C. M. *J. Phys. Chem. B* **2009**, *113*, 13134.
(124) Roland, C. M.; Fragiadakis, D.; Coslovich, D.; Capaccioli, S.; Ngai, K. L. *J. Chem. Phys.* **2010**, in press.
(125) Stillinger, F. H.; Weber, T. A. *Science* **1984**, *225*, 983.
(126) Sampoli, M.; Benassi, P.; Eramo, R.; Angelani, L.; Ruocco, G. *J. Phys.: Condens. Matter* **2003**, *15*, S1227.
(127) (a) Jones, J. E. *Proc. R. Soc. London. A* **1924**, *106*, 441. (b) *Ibid.* **1924**, *106*, 462.
(128) Dobson, J. F.; McLennan, K.; Rubio, A.; Wang, J.; Gould, T.; Le, H. M.; Dinte, B. P. *Aust. J. Chem.* **2001**, *54*, 513.
(129) Moelwyn-Hughes, E. A. *Physical Chemistry*, 2nd ed.; Pergamon Press: New York, 1961.
(130) Bardik, V. Y.; Sysoev, V. M. *Low Temp. Phys.* **1998**, *24*, 601.
(131) Widom, B. *Physica A* **1999**, *263*, 500.
(132) Widom, B. *Science* **1967**, *157*, 375.
(133) Chandler, D.; Weeks, J. D.; Andersen, H. C. *Science* **1983**, *220*, 4599.
(134) Weeks, J. D.; Chandler, D.; Andersen, H. C. *J. Chem. Phys.* **1971**, *54*, 5237.
(135) Tölle, A.; Schober, H.; Wuttke, J.; Randl, O. G.; Fujara, F. *Phys. Rev. Lett.* **1998**, *80*, 2374.
(136) Longuet-Higgins, H. C.; Widom, B. *Mol. Phys.* **1964**, *8*, 549.
(137) Speedy, R. J. *J. Phys.: Condens. Matter* **2003**, *15*, S1243.
(138) Shell, M. S.; Debenedetti, P. G.; La Nave, E.; Sciortino, F. *J. Chem. Phys.* **2003**, *118*, 8821.
(139) Hoover, W. G.; Ross, M. *Contemp. Phys.* **1971**, *12*, 339.
(140) Hiwatari, Y.; Matsuda, H.; Ogawa, T.; Ogita, N.; Ueda, A. *Prog. Theor. Phys.* **1974**, *52*, 1105.

(141) Roland, C. M.; Feldman, J. L.; Casalini, R. *J. Non-Cryst. Solids* **2006**, *352*, 4895.
(142) Grzybowski, A.; Paluch, M.; Grzybowska, K. *J. Phys. Chem. B* **2009**, *113*, 7419.
(143) Bailey, N. P.; Pedersen, U. R.; Gnan, N.; Schroder, T. B.; Dyre, J. C. *J. Chem. Phys.* **2008**, *129*, 184508.
(144) Ellison, C. J.; Mundra, M. K.; Torkelson, J. M. *Macromolecules* **2005**, *38*, 1767.
(145) Schroeder, M. J.; Roland, C. M. *Macromolecules* **2002**, *35*, 2676.
(146) Reinsberg, S. A.; Qiu, X. H.; Wilhelm, M.; Spiess, H. W.; Ediger, M. D. *J. Chem. Phys.* **2001**, *114*, 7299.
(147) Tracht, U.; Wilhelm, M.; Heuer, A.; Spiess, H. W. *J. Magn. Reson.* **1999**, *140*, 460.
(148) Tolle, A. *Rep. Prog. Phys.* **2001**, *64*, 1473.
(149) Hollander, A. G. S.; Prins, K. O. *J. Non-Cryst. Solids* **2001**, *286*, 1.
(150) Casalini, R.; Roland, C. M. *Phys. Rev. E* **2004**, *69*, 062501.
(151) Dreyfus, C.; Le Grand, A.; Gapinski, J.; Steffen, W.; Patkowski, A. *Eur. Phys. J.* **2004**, *42*, 309.
(152) Alba-Simionseco, C.; Cailliaux, A.; Alegria, A.; Tarjus, G. *Europhys. Lett.* **2004**, *68*, 58.
(153) Strictly speaking, the scaling property only applies to reduced quantities, e.g., $\tau_\alpha^{red} = \tau_\alpha(\rho^{1/3}T^{1/2})$;[137] however, in the supercooled regime the difference is negligible.
(154) Coslovich, D.; Roland, C. M. *J. Phys. Chem. B* **2008**, *112*, 1329.
(155) Tsolou, G.; Harmandaris, V. A.; Mavrantzas, V. G. *J. Chem. Phys.* **2006**, *124*, 084906.
(156) Roland, C. M.; Bair, S.; Casalini, R. *J. Chem. Phys.* **2006**, *125*, 124508.
(157) Bailey, N. P.; Pedersen, U. R.; Gnan, N.; Schroder, T. B.; Dyre, J. C. *J. Chem. Phys.* **2008**, *129*, 184507.
(158) Gnan, N.; Schroder, T. B.; Pedersen, U. R.; Bailey, N. P.; Dyre, J. C. *J. Chem. Phys.* **2009**, *131*, 234503.
(159) Coslovich, D.; Roland, C. M. *J. Chem. Phys.* **2009**, *130*, 014508.
(160) Johari, G. P.; Goldstein, M. *J. Phys. Chem.* **1970**, *74*, 2034.
(161) Bershstein, V. A.; Yegorov, V. M. *Polym. Sci. USSR* **1985**, *27*, 2743.
(162) Ngai, K. L.; Paluch, M. *J. Chem. Phys.* **2004**, *120*, 857.
(163) Schmidt-Rohr, K.; Kulik, A. S.; Beckham, H. W.; Ohlemacher, A.; Pawelzik, U.; Boeffel, C.; Spiess, H. W. *Macromolecules* **1994**, *27*, 4733.
(164) Kuebler, S. C.; Schaefer, D. J.; Boeffel, C.; Pawelzik, U.; Spiess, H. W. *Macromolecules* **1997**, *30*, 6597.
(165) Bohmer, R.; Diezemann, G.; Geil, B.; Hinze, G.; Nowaczyk, A.; Winterlich, M. *Phys. Rev. Lett.* **2006**, *97*, 135701.
(166) Ngai, K. L. *J. Chem. Phys.* **1998**, *109*, 6982.
(167) Weidersich, J.; Blochowicz, T.; Benkhof, S.; Kudlik, A.; Surovtsev, N. V.; Tschirwitz, C.; Novikov, V. N.; Rossler, E. *J. Phys.: Condens. Matter* **1999**, *11*, A147.
(168) Mierzwa, M.; Pawlus, S.; Kaminaka, E.; Paluch, M.; Ngai, K. L. *J. Chem. Phys.* **2008**, *128*, 044512.
(169) Kessairi, K.; Capaccioli, S.; Prevosto, D.; Lucchesi, M.; Sharifi, S.; Rolla, P. A. *J. Phys. Chem. B* **2008**, *112*, 4470.
(170) Prevosto, D.; Capaccioli, S.; Sharifi, S.; Lucchesi, M.; Rolla, P. A. *J. Non-Cryst. Solids* **2007**, *353*, 4278.
(171) Kudlik, A.; Benkhof, S.; Blochowicz, T.; Tschirwitz, C.; Rossler, E. *J. Mol. Struct.* **1999**, *479*, 201.
(172) Ngai, K. L.; Capaccioli, S. *Phys. Rev. E* **2004**, *69*, 031501.
(173) Penn, R. W.; Kearsley, E. A. *Trans. Soc. Rheol.* **1976**, *20*, 227.
(174) Flory, A. L.; McKenna, G. B. *Polymer* **2005**, *46*, 5211.
(175) Mott, P. H.; Argon, A. S.; Suter, U. W. *Philos. Mag. A* **1993**, *67*, 931.
(176) Roland, C. M.; Schroeder, M. J.; Fontanella, J. J.; Ngai, K. L. *Macromolecules* **2004**, *37*, 2630.
(177) Schroeder, M. J.; Ngai, K. L.; Roland, C. M. *J. Polym. Sci., Polym. Phys. Ed.* **2007**, *45*, 342.
(178) Ngai, K. L. *Philos. Mag.* **2004**, *84*, 1341.
(179) Zorn, R.; Frick, B. *J. Chem. Phys.* **1998**, *108*, 3327.
(180) Frick, B.; Richter, D. *Phys. Rev. B* **1993**, *47*, 14795.
(181) Buchenau, U.; Wischnewski, A.; Richter, D.; Frick, B. *Phys. Rev. Lett.* **1996**, *77*, 4035.
(182) (a) Hall, R. W.; Wolynes, P. G. *J. Chem. Phys.* **1987**, *86*, 2943. (b) Xia, X.; Wolynes, P. G. *Proc. Natl. Acad. Sci. U.S.A.* **2000**, *97*, 2990.
(183) Kanaya, T.; Tsukushi, T.; Kaji, K.; Bartos, J.; Kristiak, J. *Phys. Rev. E* **1999**, *60*, 1906.
(184) Sokolov, A. P.; Kisliuk, A.; Novikov, V. N.; Ngai, K. L. *Phys. Rev. B* **2001**, *63*, 172204.
(185) Larinin, L.; Ottochian, A.; De Michele, C.; Leporini, D. *Nature Phys.* **2008**, *4*, 42.
(186) Scopigno, T.; Ruocco, G.; Sette, F.; Monaco, G. *Science* **2003**, *302*, 849.
(187) Scopigno, T.; Cangialosi, D.; Ruocco, G. *Phys. Rev. B* **2010**, *81*, 100202.
(188) Hong, L.; Begen, B.; Kisliuk, A.; Alba-Simionesco, C.; Novikov, V. N.; Sokolov, A. P. *Phys. Rev. B* **2008**, *78*, 134201.
(189) Silbert, L. E.; Liu, A. J.; Nagel, S. R. *Phys. Rev. Lett.* **2005**, *95*, 098301.
(190) Leonforte, F.; Tanguy, A.; Wittmer, J. P.; Barrat, J.-L. *Phys. Rev. Lett.* **2006**, *97*, 055501.
(191) Kauzmann, W. *Chem. Rev.* **1948**, *43*, 219.
(192) Dhinojwala, A.; Wong, G. K.; Torkelson, J. M. *J. Chem. Phys.* **1994**, *100*, 6046.
(193) Casalini, R.; Roland, C. M. *Phys. Rev. Lett.* **2009**, *102*, 035701.
(194) Casalini, R.; Roland, C. M. *J. Non-Cryst. Solids* **2010**, in press.
(195) Dawson, K. J.; Kearns, K. L.; Yu, L.; Steffen, W.; Ediger, M. D. *Proc. Natl. Acad. Sci. U.S.A.* **2009**, *106*, 15165.
(196) Swallen, S. F.; Windsor, K.; McMahon, R. J.; Ediger, M. D.; Mates, T. E. *J. Phys. Chem. B* **2010**, *114*, 2635.
(197) Johari, G. P. *J. Chem. Phys.* **1982**, *77*, 4619.
(198) Yardimci, H.; Lehenya, R. L. *J. Chem. Phys.* **2006**, *124*, 214503.
(199) Adrjanowicz, K.; Paluch, M.; Ngai, K. L. *J. Phys.: Condens. Matter* **2010**, *22*, 125902.
(200) Findley, W. N.; Lai, J. S.; Onaren, K. *Creep and Relaxation of Nonlinear Viscoelastic Materials*; North-Holland Publishing: Amsterdam, 1976.
(201) Robertson, R. E. *J. Chem. Phys.* **1966**, *44*, 3950.
(202) Boyce, M. C.; Parks, D. M.; Argon, A. S. *Mech. Mater.* **1988**, *7*, 15.
(203) Struik, L. C. E. *Physical Aging in Amorphous Polymers and Other Materials*; Elsevier: New York, 1978.
(204) Yee, A. F.; Bankert, R. J.; Ngai, K. L.; Rendell, R. W. *J. Polym. Sci., Polym. Phys. Ed.* **1988**, *26*, 2463.
(205) Lee, H.-N.; Paeng, K.; Swallen, S. F.; Ediger, M. D. *Science* **2009**, *323*, 231.
(206) Ngai, K. L.; Roland, C. M. *Macromolecules* **1994**, *27*, 2454.
(207) Erman, B.; Mark, J. E. *Structures and Properties of Rubberlike Network*; Oxford University Press: New York, 1997.
(208) Alcoutlabi, M.; McKenna, G. B. *J. Phys.: Condens. Matter* **2005**, *17*, R461.
(209) Roth, C. B.; Dutcher, J. R. *J. Electroanal. Chem.* **2005**, *584*, 13.
(210) Jackson, C. L.; McKenna, G. B. *J. Non-Cryst. Solids* **1991**, *131−133*, 221.
(211) Schonhals, A.; Goering, H.; Schick, C.; Frick, B.; Mayorova, M.; Zorn, R. *Eur. Phys. J. Spec. Top.* **2007**, *141*, 255.
(212) Koppensteiner, J.; Schranz, W.; Carpenter, M. A. *Phys. Rev. B* **2010**, *81*, 024202.
(213) Le Quellec, C.; Dosseh, G.; Audonnet, F.; Brodie-Linder, N.; Alba-Simionesco, C.; Haussler, W.; Frick, B. *Eur. Phys. J. Spec. Top.* **2007**, *141*, 11.
(214) He, F.; Wang, L.-M.; Richert, R. *Phys. Rev. B* **2005**, *71*, 144205.
(215) Akabori, K.-I.; Tanaka, K.; Takahara, A.; Kajiyama, T.; Nagamura, T. *Eur. Phys. J. Spec. Top.* **2007**, *141*, 173.
(216) Forrest, J. A.; Mattsson, J. *Phys. Rev. E* **2000**, *61*, R53.
(217) Ellison, C. J.; Torkelson, J. M. *Nature Mater.* **2003**, *2*, 695.
(218) Priestley, R. D.; Ellison, C. J.; Broadbelt, L. J.; Torkelson, J. M. *Science* **2005**, *309*, 456.
(219) Inoue, R.; Kanaya1, T.; Nishida, K.; Tsukushi, I.; Taylor, J.; Levett, S.; Gabrys, B. J. *Eur. Phys. J. E* **2007**, *24*, 55.
(220) He, F.; Wang, L.-M.; Richert, R. *Eur. Phys. J. Spec. Top.* **2007**, *141*, 3.
(221) Ngai, K. L. *J. Polym. Sci., Polym. Phys. Ed.* **2006**, *44*, 2980.
(222) Forrest, J. A.; Dalnoki-Veress, K. *Adv. Colloid Interface Sci.* **2001**, *94*, 167.
(223) Roth, C. B.; Pound, A.; Kamp, S. W.; Murray, C. A.; Dutcher, J. R. *Eur. Phys. J. E* **2006**, *20*, 441.
(224) Campbell, C. G.; Vogt, B. D. *Polymer* **2007**, *48*, 7169.
(225) Fukao, K. *Eur. Phys. J. E* **2003**, *12*, 119.
(226) Tran, T. A.; Said, S.; Grohens, Y. *Composites: Part A* **2005**, *36*, 461.
(227) Roth, C. B.; Torkelson, J. M. *Macromolecules* **2007**, *40*, 3328.
(228) Robertson, C. G.; Hogan, T. E.; Rackaitis, M.; Puskas, J. E.; Wang, X. *J. Chem. Phys.* **2010**, *132*, 104904.
(229) Bansal, A.; Yang, H.; Li, C.; Cho, K.; Benicewicz, B. C.; Kumar, S. K.; Schadler, L. S. *Nature Mater.* **2005**, *4*, 693.
(230) Ash, B. J.; Schadler, L. S.; Siegel, R. W. *Mater. Lett.* **2002**, *55*, 83.

(231) Oh, H.; Green, P. F. *Nature Mater.* **2008**, *8*, 139.
(232) Elmahdy, M. M.; Chrissopoulou, K.; Afratis, A.; Floudas, G.; Anastasiadis, S. H. *Macromolecules* **2006**, *39*, 5170.
(233) Robertson, C. G.; Roland, C. M. *Rubber Chem. Technol.* **2008**, *81*, 506.
(234) Harton, S. E.; Kumar, S. K.; Yang, H.; Koga, T.; Hicks, K.; Lee, H. K.; Mijovic, J.; Liu, M.; Vallery, R. S.; Gidley, D. W. *Macromolecules* **2010**, *43*, 3415.
(235) Sen, S.; Xie, Y.; Bansal, A.; Yang, H.; Cho, K.; Schadler, L. S.; Kumar, S. K. *Eur. Phys. J. Spec. Top.* **2007**, *141*, 161.
(236) He, F.; Wang, L.-M.; Richert, R. *Phys. Rev. B* **2005**, *71*, 144205.
(237) Bogoslovov, R. B.; Roland, C. M.; Ellis, A. R.; Randall, A. M.; Robertson, C. G. *Macromolecules* **2008**, *41*, 1289.
(238) McKenna, G. B. *J. Phys. IV* **2000**, *10*, Pr7–53.
(239) Grohens, Y.; Hamon, L.; Reiter, G.; Soldera, A.; Holl, Y. *Eur. Phys. J. E* **2002**, *8*, 217.
(240) Fakhraai, Z.; Sharp, J. S.; Forrest, J. A. *J. Polym. Sci., Polym. Phys. Ed.* **2004**, *42*, 4503.
(241) Huth, H.; Minakov, A. A.; Serghei, A.; Kremer, F.; Schick, C. *Eur. Phys. J. Spec. Top.* **2007**, *141*, 153.
(242) Koh, Y. P.; Simon, S. L. *J. Polym. Sci., Polym. Phys. Ed.* **2008**, *46*, 2741.
(243) Serghei, A.; Chen, D.; Lee, D. H.; Russell, T. P. *Soft Matter* **2010**, *6*, 1111.
(244) Serghei, A.; Tress, M.; Kremer, F. *J. Chem. Phys.* **2009**, *131*, 154904.
(245) Schonhals, A.; Goering, H.; Schick, C.; Frick, B.; Zorn, R. *Eur. Phys. J. E* **2003**, *12*, 173.
(246) Soles, C. L.; Douglas, J. F.; Jones, R. L.; Wu, W.-L. *Macromolecules* **2004**, *37*, 2890.
(247) Inoue, R.; Kanaya, T.; Nishida, K.; Tsukushi, I.; Shibata, K. *Phys. Rev. Lett.* **2005**, *95*, 056102.